Photoinduced Linkage Isomers of Transition-Metal Nitrosyl Compounds and Related Complexes

Philip Coppens,* Irina Novozhilova, and Andrey Kovalevsky

Department of Chemistry, State University of New York at Buffalo, Buffalo, New York 14260-3000

Received September 18, 2001

Contents

* To whom correspondence should be addressed. E-mail: coppens@acsu.buffalo.edu.

I. Introduction

The seminal discovery of light-induced changes in transition-metal nitrosyl complexes in the late 1970s and their identification as metastable linkage isomers almost 20 years after the initial discoveries have in recent years motivated a plethora of experimental and theoretical studies. They have raised the question of whether the linkage isomers play a role in the many crucial biological processes involving nitric oxide, which though likely, is still a subject of investigation. The linkage isomers have potential technological importance, as the change in refractive index on a molecular scale, associated with the photoinduced change in the crystals, in principle allows the design of very high capacity storage devices.

This review summarizes the current knowledge in the still-developing field and includes a discussion of photoinduced metastable linkage isomers of related substances.

II. Photocrystallography

A. Crystallography of Light-Induced Species

Unlike in solution or in the gas-phase, molecules in crystals generally have a well-defined geometry, and their relative orientation is dictated by packing forces. The study of photoinduced processes in crystals thus offers a unique possibility for elucidating detailed geometry changes at the atomic level, provided crystallinity is preserved at a reasonable degree of conversion to the photoinduced species. Such work is a logical extension of pioneering studies by Schmidt and co-workers in the 1960s and 1970s,[1] who showed that the products of intermolecular photoinduced solid-state reactions are topochemically controlled by the relative arrangements of the reactive centers in the crystal.

In *photocrystallography*, spectroscopic and crystallographic techniques are combined to allow the study of light-induced metastable and transient species. The sample is irradiated in situ on the X-ray diffractometer and generally cooled using either cryostatic or gas flow techniques. If the light-induced species is sufficiently stable, which is the case for many of the linkage isomers, irradiation can precede diffraction, which has the advantage that a temperature increase due to dissipation of the laser power is avoided during the diffraction experiment. If the light-induced species has a very short lifetime of, say

10.1021/cr000031c CCC: $39.75
Published on Web 02/13/2002

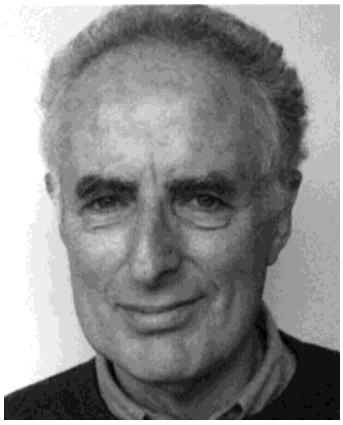

Philip Coppens received his Ph. D. from the University of Amsterdam and has since been employed at the Weizmann Institute of Science, Brookhaven National Laboratory, and the State University of New York at Buffalo, where he is currently Distinguished Professor of Chemistry. He is a Corresponding Member of the Royal Dutch Academy of Sciences and a Doctor Honoris Causa of the University of Nancy, France. He is a Past President of the American Crystallographic Association and served as President of the International Union of Crystallography from 1993 to 1996. Among his awards are the Gregori Aminoff Prize of the Royal Swedish Academy of Sciences and the Martin Buerger Award of the American Crystallographic Association. His research interests include X-ray charge density analysis, synchrotron radiation crystallography, and photocrystallography, the study of light-induced metastable and transient species in crystals, the latter by use of time-resolved diffraction, and, in general, the combination of experimental results with parallel quantum mechanical calculatons. His most recent book, entitled *X-ray Charge Densities and Chemical Bonding*, was published in 1997.

Irina Novozhilova was born in St. Petersburg, Russia. She received her B.Sc. in Geochemistry/Crystallography in 1995 from St.-Petersburg State University under the guidance of Dr. E. V. Kir′yanova and Prof. O. V. Frank-Kamenetskaya. In 1996, she joined Prof. Philip Coppens' research group at the State University of New York at Buffalo, where she received an M.A. in Physical Chemistry in 2000 and is currently pursuing a Ph.D. degree. Her research concerns the quantum mechanical study of photoinduced long-lived metastable and excited states of transition-metal complexes. Her major research interest involves the application of computational methods in physical chemistry.

milliseconds or less, and reverts to the ground state after excitation, a stroboscopic experiment can be performed, in which a pulsed laser source is combined with a pulsed X-ray probe source.[2,3] We will discuss the latter type of experiments elsewhere, as they are not necessary for the longer-lived nitric oxide coordination species.

Even in the case of light-induced metastable states, only part of the molecules in the crystal is converted to the new species. Thus, the diffraction experiment

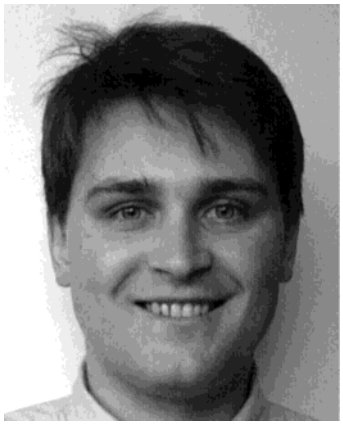

Andrey Yu. Kovalevsky was born in 1974 in Kharkov, Ukraine. He received his M.Sc. in Organic Chemistry in 1996 from the Kharkov State University under the supervision of Professors Sergey M. Desenko and Valeriy D. Orlov. From 1996 to 1999, he worked at the X-ray Structural Center of A. N. Nesmeyanov Institute of Organo-element Compounds of the Russian Academy of Sciences, Moscow, Russia, where he was involved in the study of conformational analysis of organic heterocyclic compounds. Since 1999, he has been a graduate student at the State University of New York at Buffalo in the laboratory of Professor Philip Coppens, where he is involved in the study of light-induced metastable states of transition-metal complexes containing ambidentate di- and triatomic ligands.

deals with a disordered crystal, but with the essential distinction that information on one of the components is available, as the not affected "dark" component can be determined in a prior experiment on the ground-state crystal.

In the application of both Fourier and least-squares methods in photocrystallography, information on the ground state is introduced to identify the photoinduced changes. A *photodifference* electron density map is related to the difference density maps routinely employed in crystal structure analysis, in which a calculated electron density is subtracted from the observed density by means of a Fourier series over the structure factors F at the reciprocal lattice positions defined by $\mathbf{H}$:

$$\Delta\rho(\mathbf{r}) = \frac{1}{V_{\text{cell}}}\sum_{\mathbf{H}}[F_{\text{obs}}(\mathbf{H}) - F_{\text{calc}}(\mathbf{H})]\exp(-2\pi i\mathbf{Hr}) \quad (1)$$

To obtain the photodifference map, F_{calc}, the calculated structure factor is based on the ground-state molecular geometry, converted to the fractional coordinates of the new cell to account for any change in cell dimensions, which can be a tenth of an angstrom or less depending on the conversion percentage achieved, while F_{obs}, the observed structure factor, is from the experiment after irradiation. A typical photodifference map, for [Ni(NO)(η^5-Cp*)], reproduced in Figure 1,[4] shows pronounced electron-deficient regions at the original positions of the nitrosyl atoms, and excess density along a line approximately perpendicular to the original NO direction, indicating a reorientation of the NO ligand. Negative and positive areas near the Ni position indicate a shift of the metal atom toward the diatomic ligand upon photoinduced isomerization.

As in more routine crystal structure determination, least-squares methods are needed to obtain quantita-

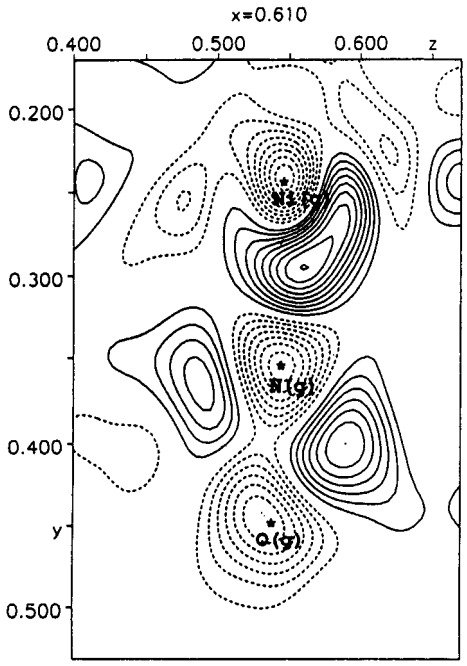

Figure 1. Difference in electron density between the photoirradiated [Ni(NO)(η^5-Cp*)] crystal and ground-state molecules. Contours at 0.4 e Å^{-3}. Negative contours dotted. (Reproduced with permission from ref 4. Copyright 1998 The American Chemical Society.)

tive results. For a crystal in which only part of the molecules are converted, the structure factor expression, assuming random distribution of the photoconverted molecules, and the presence of only two species, is

$$F = (1 - P)F'_{gs} + PF_{pi} + F_{rest} \qquad (2)$$

where the subscripts "gs" and "pi" represent the ground and photoinduced molecular states, respectively, P is the conversion percentage, and the subscript "rest" represents inert moieties such as water of crystallization or counterions not involved in the excitation. F'_{gs} may not be identical to F_{gs}, the structure factor of the ground state crystal, as the ground-state molecules may move or rotate slightly due to the changed molecular environment, which can readily be allowed for in the analysis. Thus, in general, the parameters of the refinement will be (i) those describing the geometry of the light-induced species, (ii) its population, plus (iii) parameters describing the translations and rotations of the ground-state species treated as rigid bodies. The assumption of random distribution of the light-induced species has, so far, worked well, and is supported by the absence of extra diffraction spots, which would indicate a more ordered arrangement. Slight differences in unit cell dimensions must be properly taken into account in the treatment.

B. Supporting Techniques

Though crystallography provides unique information on the geometry, alternate instrumental methods are invaluable for identification of new species prior to the diffraction experiment and for measurement of other physical properties. Foremost among these are differential scanning calorimetry (DSC) of the photoexcited sample and infrared (IR) measurement of light-induced vibrational changes.

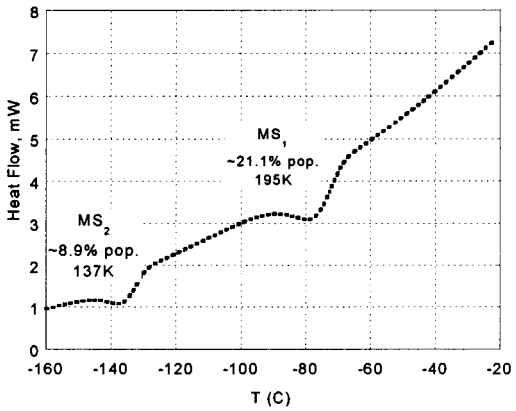

Figure 2. DSC curve for a laser-irradiated crystal of SNP. Heating rate 4 °C/min. The dips in the curve indicate heat being released by the decay of the photoinduced species (Reproduced with permission from ref 5b. Copyright 1998 The Royal Society of Chemistry.)

A DSC scan for $Na_2[Fe(CN)_5NO]\cdot 2H_2O$, sodium nitroprusside (SNP), indicating the existence of two different light-induced species, labeled MS1 and MS2, is shown in Figure 2.[5] The curves are obtained at a constant rate of temperature increase, while the heat flow to the sample, displayed in the graph, is being monitored. The dips in the curves indicate heat released upon relaxation of higher energy species to the ground state. The area of the depressions allows a quantitative evaluation of the heat being released. With the known weight of the sample, an estimate of the fractional conversion percentage can be obtained, provided the difference in enthalpy of the two states is known at least approximately.

IR of samples irradiated at low temperatures provides a rapid means of testing for the generation of new species and measurement of their decay temperatures. Selective isotope substitution allows identification of the group(s) involved, while the fractional conversion percentage can be estimated from the decrease in the original IR bands. The seminal discovery by Crichton and Rest on [Ni(NO)(η^5-Cp)],[6] which is discussed in detail below, was based on IR spectroscopic measurements.

III. Metastable Isomers of Transition-Metal Nitrosyl Complexes

A. The First Discoveries

The light-induced changes in crystals of sodium nitroprusside dihydrate $Na_2[Fe(CN)_5(NO)]\cdot 2H_2O$, or SNP, were discovered in 1977, as part of a Mössbauer spectroscopy study of optical dispersion in transparent molecular systems. When SNP was used as the medium, a new low-temperature-stable species was observed, with quadrupole splitting and isomer shift markedly different from those of the normal ground state.[7]

Subsequent DSC studies of the thermal decay of metastable states of SNP, reported in 1989, revealed not one, but at least two, light-induced species,[8] labeled MS1 and MS2, with MS2 decaying at a lower

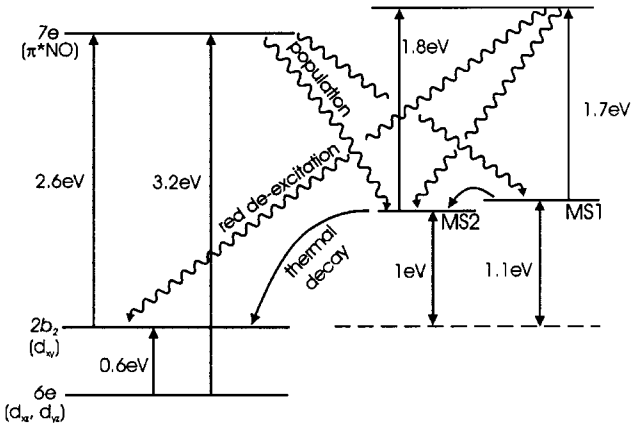

Figure 3. Relative positions of the MS1 and MS2 states of SNP, their excited states, and excited levels of the ground state, after ref 8.

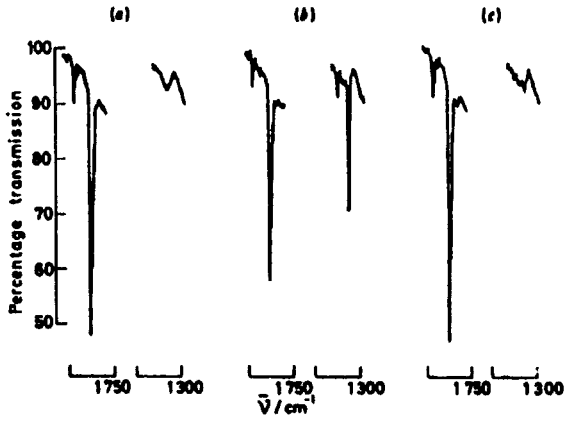

Figure 4. Infrared spectra as recorded by Crichton and Rest in 1977 of a mixture of [Ni(η-C_5H_5)(^{14}NO)] and [Ni(η-C_5H_5)(^{15}NO)] isolated in an argon matrix: (a) after deposition; (b) after photolysis for 5 min with a $230 < \lambda < 280$ nm filter; (c) after more photolysis for another 10 min with a $290 < \lambda < 350$ filter. (Reproduced with permission from ref 6. Copyright 1977 The Royal Society of Chemistry.)

temperature than MS1, as illustrated in Figure 2. Evidence for a much faster decaying species (by a factor of about 50) was also obtained,[8] but seems not to have been pursued further. The decay follows first-order kinetics and is a single-particle effect rather than a cooperative phenomenon. From the DSC measurements on a sample of known (45%) MS1 conversion percentage, the energy difference between this state and the ground state (GS) has been calculated as 1.1 eV. Combining this number with the energy of the absorption bands of MS1 and MS2 leads to a value of 1.0 eV of the position of MS2 above the GS level.[8] The relative positions of MS1 and MS2, their excited states, and excited levels of the ground state, as calculated semiempirically in early work by Manoharan and Gray,[9] are schematically depicted in Figure 3. The initial transition is an electronic excitation from the ground-state HOMO, $2b_2$ (d_{xy}) orbital to the LUMO, 7e (π*NO) orbital (using the approximate C_{4v} point group symmetry),[10] with the excited species subsequently relaxing into one of the metastable states.

The saturation population is strongly dependent on the direction of polarization of the exciting light and can be as high as 50% for MS1 for light polarized along the c-direction of the crystal.[11] The crystals of SNP are orthorhombic (space group *Pnnm*) and contain molecules with two different orientations of the NC−Fe−NO molecular pseudosymmetry axis (the molecular point group is almost C_{4v}). The two axes lie in the mirror plane, inclined at about +37° and −37°, respectively, to the crystallographic *a*-axis. It was noted that the MS2 state reaches saturation substantially quicker than the MS1 state,[11] an observation that can be understood in terms of the linkage isomer interpretation, according to which the MS2 state is an intermediate along the GS → MS1 reaction coordinate, as described in detail below.

In the same year as the discovery of the light-induced metastable states of SNP, but apparently quite unrelated, Rest and co-workers observed new light-induced absorption bands in the IR spectrum of [Ni(NO)(η^5-Cp)].[6] They found that irradiation of the sample embedded in inert matrixes (Ar, CH_4, and N_2) at 20 K with ultraviolet light ($230 < \lambda < 280$ nm) caused a 40% reduction of the intensity of the NO stretching band at 1839 cm^{-1} and the appearance of an intense new band at 1392 cm^{-1}. The new band could be bleached by continued irradiation using a filter with a $290 < \lambda < 350$ nm band-pass (Figure 4). The authors concluded that electron transfer from the metal to the nitrosyl ligand was involved, with possible bending of the M−N−O group. The metastable state, later identified as MS2-type, decays at a much lower temperature (∼50 K) than the MS2 state of SNP.

It is noticeable that the almost simultaneous discoveries concern complexes with very different electronic states. In the classification of Enemark and Feltham,[12] which counts the number of d-electrons on the metal atom plus the number of antibonding electrons on the nitrosyl ligand, thus avoiding an ambiguous distinction, SNP is an {MNO}^{6} complex, while Ni(NO)Cp is {MNO}.[10] It has now become evident that in both cases very similar linkage isomers are generated and that the generation of linkage isomers upon light exposure is a quite common occurrence in nitrosyl chemistry. Subsequent studies confirm that photoinduced linkage isomerization is not limited to nitrosyl compounds but also occurs in many other complexes in which small di- or triatomic ligands are bonded to transition-metal atoms, as discussed further in section V.

B. The Nature of the Metastable States of Sodium Nitroprusside

1. Sodium Nitroprusside (SNP): Experimental Details

In the 1977 publications, the new species were described as a new isomeric molecular state, with energies close to that of the ground state and very likely diamagnetic. In later work, the terms "long-lived electronic states" and "intramolecular electronic excitations" were used, with the new species being described as relaxed derivatives arising from a metal-to-ligand (Fe → NO) charge transfer[8,13] or, in an alternative proposal, from a d → d transition confined to the metal atom.[14] But as was pointed out by Güdel,[15] the longevity of the metastable states is

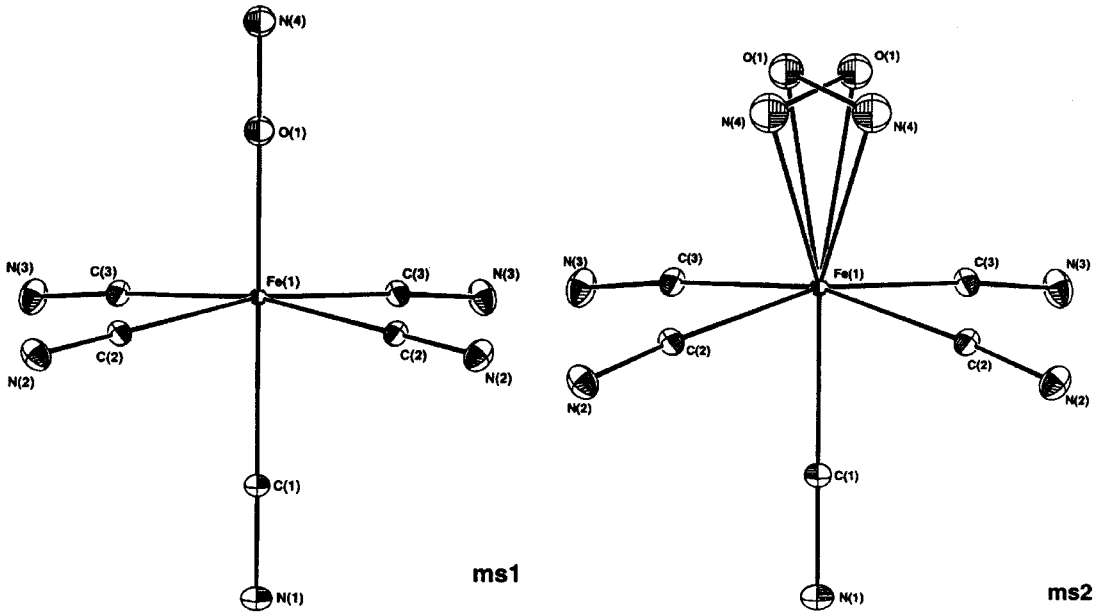

Figure 5. ORTEP plots of the MS1 and MS2 linkage isomers of SNP at 50 K; 50% probability ellipsoids. (Reproduced with permission from ref 5. Copyright 1997 The American Chemical Society.)

Table 1. Structural Parameters of the Ground State of the SNP Anion (Bond Lengths in Å, Angles in deg)

	LDA		GGA		
	Dirac-VWN[a]	PWC[b]	B88P86[a]	B3LYP[c]	expt 50 K[d]
Fe−N	1.616	1.624	1.642	1.624	1.6656(7)
N−O	1.159	1.158	1.170	1.143	1.1331(10)
$Fe-C_{ax}$	1.915	1.914	1.957	1.970	1.9257(9)
$Fe-C_{eq}$	1.907	1.915	1.959	1.972	1.9310/1.9403(6)
$C-N_{ax}$	1.164	1.169	1.172	1.159	1.1591(12)
$C-N_{eq}$	1.166	1.170	1.173	1.159	1.1603/1.1622(8)
$\angle Fe-C-N_{ax}$	180.0		180.0		179.78(8)
$\angle Fe-C-N_{eq}$	175.0		175.0		178.34/176.49(6)
∠Fe−N−O	180.0	180.0	180.0	180.0	176.03(7)
$\angle N-Fe-C_{ax}$	180.0	180.0	180.0		176.63(4)
$\angle N-Fe-C_{eq}$	95.2		94.5		93.40/97.65(2)
$\angle C_{eq}-Fe-C_{eq(trans)}$	169.6		171.1		168.91(3)
$\angle C_{eq}-Fe-C_{eq(cis)}$	89.5		89.7		90.25/88.20(2)

[a] Reference 34. [b] Reference 33. [c] Reference 65. [d] Reference 5.

inconsistent with any one-electron-transfer model, either a large structural change or a multielectron promotion is required to explain the stability of the species. Mössbauer[16] and ESR[17] evidence confirmed that both MS1 and MS2 are diamagnetic, thus ruling out a spin-forbidden transition, in agreement with the observation that decay of the metastable states is radiationless.

The first indication that an atomic rearrangement was involved came from the photocrystallographic study reported in 1994.[18] When data collected on a photoexcited crystal of SNP were subjected to a charge-density refinement, more electrons were found on the proximal atom than on the distant atom of the NO group. This observation was supported by the result of a least-squares refinements of the light-induced state, which produced a large anomaly for the atomic displacement parameters when the N-bound geometry was selected, with the terminal atom having mean-square displacements up to 20 times larger than those of the proximal atom, indicating an incorrect element assignment.[19] Similar results were subsequently obtained for $K_2[RuNO(NO_2)_4OH]$[20] and other complexes. Further analysis using photo-difference maps, like the one shown in Figure 1, and least-squares techniques, revealed that MS1 and MS2 are isonitrosyl (η^1-O) and side-bound (η^2-NO) linkage isomers, not previously observed for NO, though an oxygen-bound isomer was known for the nitro group, as discussed in Section V. ORTEP plots of the MS1 and MS2 linkage isomers of SNP are shown in Figure 5.

The 50 K bond lengths and angles in the ground state and in the two metastable states of SNP are summarized in Tables 1−3, together with theoretical results discussed further below. Geometric changes upon transition to MS_1 are the lengthening of the bond from the iron atom to the proximal atom of the NO ligand (N for the GS, O for MS1) by 0.053(6) Å, accompanied by a cooperative change in the angles between the trans equatorial ligands, which increase slightly from 168.91(3)° to 170.0(3)°, a change in accordance with the diminished 1−3 (i.e., between two atoms two bonds apart) repulsion with the proximal atom of the nitrosyl ligand. In MS2, on the other hand, the equatorial ligands are repelled by the

Table 2. Structural Parameters of the Metastable State MS1 of the SNP Anion (Bond Lengths in Å, Angles in deg)

	LDA		GGA		
	Dirac-VWN[a]	PWC[b]	B88P86[a]	B3LYP[c]	expt 50 K[d]
Fe−O	1.697	1.700	1.731	1.713	1.175(5)
N−O	1.151	1.148	1.163	1.129	1.140(7)
$Fe-C_{ax}$	1.875	1.880	1.921	1.929	1.926(6)
$Fe-C_{eq}$	1.906	1.914	1.960	1.975	1.940/1.947(4)
$C-N_{ax}$	1.166	1.170	1.172	1.159	1.149(7)
$C-N_{eq}$	1.168	1.171	1.175	1.159	1.154/1.161(4)
$\angle Fe-C-N_{ax}$	180.0		180.0		179.3(4)
$\angle Fe-C-N_{eq}$	175.2		175.5		178.6/176.6(3)
∠Fe−O−N	180.0		180.0	180.0	174.9(4)
$\angle O-Fe-C_{ax}$	180.0	180.0	180.0		177.1(3)
$\angle O-Fe-C_{eq}$	94.3		93.6		93.0/97.0(2)
$\angle C_{eq}-Fe-C_{eq(trans)}$	171.3		172.9		170.0(3)
$\angle C_{eq}-Fe-C_{eq(cis)}$	89.7		89.8		90.1(2), 88.5(1)

[a] Reference 34. [b] Reference 33. [c] Reference 65. [d] Reference 5.

Table 3. Structural Parameters of the Metastable State MS2 of the SNP Anion (Bond Lengths in Å, Angles in deg)

	LDA		GGA		
	Dirac-VWN[a]	PWC[b]	B88P86[a]	B3LYP[c]	expt 50 K[d]
Fe−N	1.794	1.812	1.834	1.850	1.893(19)
Fe−O	1.989	2.005	2.057	2.018	2.067(15)
N−O	1.204	1.192	1.210	1.171	1.14(2)
$Fe-C_{ax}$	1.871	1.877	1.917	1.925	1.820(13)
$Fe-C_{eq}$		1.914, 1.930, 1.930, 1.911		1.963, 1.969, 1.992	1.938/1.958(8)
$C-N_{ax}$		1.170		1.159	1.160
$C-N_{eq}$		1.170, 1.171		1.159	1.160
$\angle Fe-C-N_{ax}$					176.6(11)
$\angle Fe-C-N_{eq}$					175.9(10), 174.8(8)
∠Fe−N−O	80.5	80.9	82.2	80.4	82.0(13)
$\angle N-Fe-C_{ax}$	155.6	154.7	155.3	156.1	158.7(6)

[a] Reference 34. [b] Reference 33. [c] Reference 65. [d] Reference 5.

side-on NO group, and the $C_{eq}-Fe-C_{eq(trans)}$ angle decreases from 168.91(3)° to 165.4(5)°. The Fe−C(axial) bond is considerably shortened in MS2 (but not in MS1) by 0.106(14) Å. The N−O bond lengths, on the other hand, are surprisingly little changed from the ground-state value.

Spectroscopic results are in agreement with the linkage-isomer assignment. The Raman study of Morioka et al.[21] shows a downshift from 669 to 655 cm^{-1} of the δ(Fe−N−O) band of the ground state upon ^{15}NO substitution, while the corresponding band for MS1 at 582 cm^{-1} shifts by only 1 cm^{-1}, as expected if the NO ligand in MS1 is bound through the oxygen atom, and in agreement with calculated downshifts for the GS and the isonitrosyl MS1 structures. An infrared study, including also ^{18}O isotopic substitution, leads to the same conclusion,[22] the $^{16/18}O$ isotope shift of the δ(Fe−X−Y) bending mode being *larger* for MS1 than for the ground-state species.

Thus, though the X-ray results on SNP were not universally accepted at first, as neutron diffraction studies have been inconclusive,[23] and early spectroscopic results were interpreted differently,[24] they are now supported by both spectroscopic results and a series of theoretical calculations from different laboratories, as described in sections III.B.3, III.C.1, III.C.4, IV.B, and IV.C below.[25]

2. Orbital Ordering of the SNP Ground-State Species

Though the electronic structure of SNP has been studied extensively, the nature of its HOMO has not been unambiguously established. The first theoretical analysis was carried out by Manoharan and Gray[9] using the experimental ground-state geometry of $[Fe(CN)_5NO]^{2-}$ of Manoharan and Hamilton.[26] The SCCC (self-consistent charge and configuration)−MO method gave the ordering and occupancy of the molecular orbitals as $7e(d_{xz},d_{yz})^4 2b_2(d_{xy})^2 7e(\pi^*NO)^0 3b_1(d_{x^2-y^2})^0 5a_1(d_{z^2})^0$. Accordingly, the π^*(NO) LUMO is situated between the metal d_{xy} and $d_{x^2-y^2}$ orbitals, and the low-energy absorption bands are charge-transfer (CT) transitions from the metal e and b_2 levels to the π^*(NO) orbital. Fenske−Hall-type calculations[27] of SNP and other first-row transition-metal nitrosylpentacyanides similarly indicated the HOMO to be a b_2 orbital of mostly metal d_{xy} character with some $\pi(CN_{cis})$ contribution. The assignment was compatible with the interpretation of a variety of experimental results obtained with the ESR,[28] XPS,[26] XANES,[18] polarized absorption,[9,26] and Mössbauer[28] techniques.

However, the low energy excitations of SNP have rather weak intensity, which would be unusual for CT bands in this type of compounds, which should correspond to strong bands in the absorption spectrum. Subsequent semiempirical INDO calculations by Bottomley and Grein[29] gave a different picture and indicated the HOMO to be a π orbital localized on

Table 4. Summary of Spacing of Energy Levels (eV) of the Frontier-Molecular Orbitals of the SNP Anion at Different Levels of Theory

orbital	HF-CISD, GTO[a]	DFT, PW91, DND[b]	DFT, B88P86, STO[c]	DFT, B88P86, STO[d]
HOMO-1	0.34	0.54	0.89	0.87
HOMO	9.46	2.29	1.98	2.01
LUMO	1.93	2.20	1.55	1.60
LUMO+1				

[a] Reference 28. [b] Reference 33. [c] Reference 34. [d] Reference 35.

the CN ligands and the metal d-orbitals to be located several eV below the Fermi level. They are qualitatively supported by SINDO calculations of Golebiewski and Wasiliewska[30] and Wasielewska,[31] though according to the latter calculations the HOMO has 40% metal character plus a contribution from the equatorial CN ligands. All methods agree that the LUMO is a doubly degenerate orbital of mainly π^*-(NO) character.

The controversy has not been completely resolved with the advent of more sophisticated ab initio calculations. The 1994 HF calculations of Pressprich at al.[18] indicated the $b_2(d_{xy})$ orbital to be well below the HOMO level. They were set aside by the authors because of the disagreement with the experimental results listed above, though they are supported by subsequent HF results. The HF/CI−SD calculations[28] of Hollauer and Olabe assign the first electronic transition to ligand-to-ligand charge transfer from axial-cyano to the nitrosyl ligand, the e-type HOMO being composed of CN orbitals with about 70% axial-CN character. The excitation energy of $d_{xz,yz} \rightarrow \pi^*$-(NO) and $d_{xy} \rightarrow \pi^*$(NO) transitions were calculated with the ΔSCF method (including CI) as 4.52 and 5.04 eV, which is in good agreement with the spectroscopic observations. The authors assigned the lower energy bands at 2.8 and 3.1 eV to the HOMO-1 (a_1) and HOMO-3 (a_2) → LUMO transitions.

However, DFT calculations give a different orbital ordering with the HOMO having major contributions from both the metal orbitals and the equatorial cyanides. Accordingly, the lowest energy band in the UV−vis spectrum is assigned to a metal-to-ligand CT transition,[32] as in the very early calculations. Similarly, the DFT results of Delley et al.[33] give the HOMO as having b_2 symmetry, as do the recent calculations of Boulet et al.,[34] according to which the b_2 HOMO has 69% d_{xy} and 26% N_{eq} character. This is within a few percent of our own DFT results[35] with a VWN[36] local density functional, triple-ζ basis functions on Fe with a neon frozen core and a triple-ζ basis set with a polarization function added on C, N, and O atoms. A pronounced discrepancy between DFT and HF is also observed for the HOMO−LUMO energy gap, which is about 2 eV according to the DFT calculations and about 9.4 eV for the HF calculations. Some of the results are summarized in Table 4. The DFT energy level diagram is schematically depicted in Figure 6.

Thus, while the DFT and HF calculations are consistent within each method, even when the latter include CI, there is a clear discrepancy between the two sets that requires further attention.

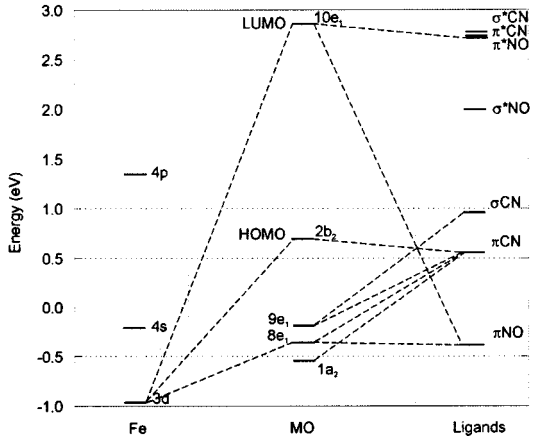

Figure 6. Partial energy-level diagram of the ground state of SNP anion as calculated by the DFT method. The left and right columns are shifted relative to the central column.

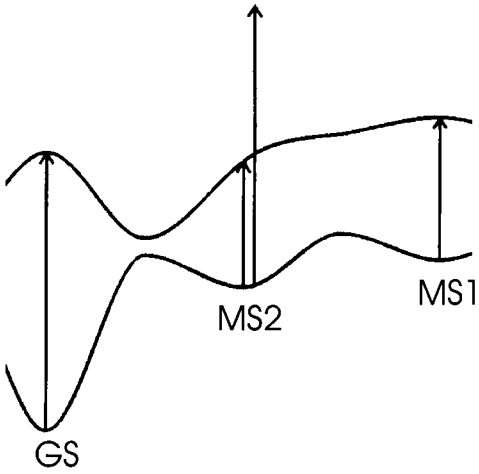

Figure 7. Calculated ground-state and relaxed excited-state potential energy surfaces of SNP along ∠FeNO reaction coordinate. (Reproduced with permission from ref 33. Copyright 1997 The American Institute of Physics.)

3. Theoretical Calculation of the Metastable and Excited States and the Mechanism of Photoinduced Interconversion

The first calculations of the metastable states of SNP using the DFT method with two different density functionals (the local PWC[37] and gradient corrected PW91[38] functionals) by Delley et al.[33] were done for both the isolated anions and the periodic crystal. They showed the ground-state potential energy surface (Figure 7) to have local minima for the sideways-bonded (MS2) and the metastable O-bound isonitrosyl (MS1) states, thus providing an explanation for the diamagnetism of the linkage isomers. The energies of the linkage isomers were

calculated to be 1.386 and 1.677 eV for MS2 and MS1, respectively, above the ground-state energy, compared with experimental values of 1.0 and 1.1 eV.[8] In the lowest energy conformation of η^2-NO (MS2a), the NO ligand is eclipsed with respect to the equatorial cyanides, while a second, locally stable, conformation, also of C_s symmetry, has the staggered (MS2b) conformation. The MS2b configuration is calculated to be 0.084 eV higher in energy than the eclipsed MS2a structure, in agreement with the crystallographic experiment, which shows the eclipsed form to exist in the solid. The ground-state potential energy surface shows two maxima corresponding to the GS → MS2 and MS2 → MS1 transition states. While the local PWC functional gives ground-state geometries in better agreement with experiment than the PW91 functional, the effect of basis set choice is not very pronounced, the observed variation in the bond lengths being only about 0.01 Å.

The excited state, created by the HOMO−LUMO $b_2 \rightarrow e$ transition, has a single electron in a doubly degenerate e orbital and undergoes a Renner−Teller lowering of the symmetry due to bending of the Fe−N−O angle. The resulting relaxed state is close in energy and geometry to the GS/MS1 transition state, thus providing an explanation for the considerable efficiency of the isomerization process.

Both the ground-state structure and the mechanism of the light-induced isomerization were studied in detail by Boulet et al.,[34,39] using both LDA (local density approximation) and GGA (generalized gradient approximation) methods, the latter with the Becke[40] exchange and Perdew[41] correlation functionals (B88P86). The ground-state results generally reproduce those of Delley et al.,[33] though the theoretical ground-state bond lengths from different methods differ in detail (Table 1). Calculation of the HOMO → LUMO excited state shows that upon Renner−Teller vibronic distortion the Fe−N−O angle is reduced to 119.1° and the Fe−N bond length increases to a value close to that of the MS2 species. The resulting geometrically relaxed excited state, labeled r-ExSt$_{GS}$, is only 0.17 eV higher in energy than the GS ↔ MS2 transition state. The vertically excited state of MS2 can relax either toward the GS or toward the MS1 metastable state in the Walsh diagram. The first relaxed state, r-ExSt$^{l}_{MS2}$, has a geometry that is essentially identical to that of r-ExSt$_{GS}$, thus accounting for the backward and forward photoinduced GS ↔ MS2 reactions. The second relaxed excited state of MS2, r-ExSt$^{r}_{MS2}$, is located toward MS1 in the Walsh diagram (see Figure 7). As its energy is calculated lower than that of the MS2 ↔ MS1 transition state and the state is located on the MS1 side of the barrier, it can account for a light-induced MS2 → MS1 transition. However, it is emphasized that the geometry and energy of the transition states may be subject to imprecision, as they are relatively crude estimates from linear transit calculations.

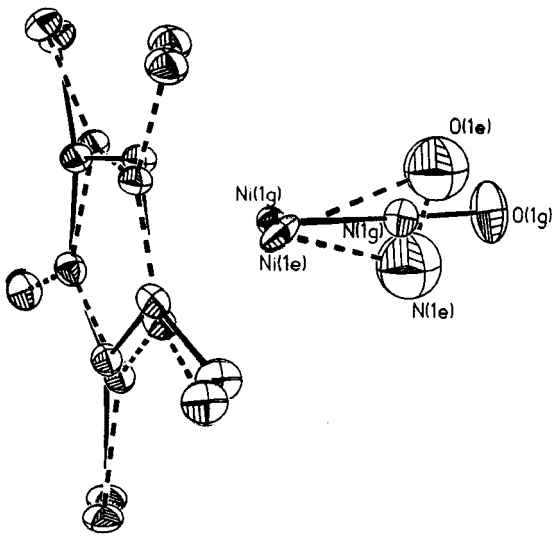

Figure 8. ORTEP drawing of one of the two crystallographically independent molecules (molecule A) of [Ni(NO)(η^5-Cp*)] in its ground and metastable states. 50% probability ellipsoids are shown. Hydrogen atoms are omitted for clarity.

C. Other Small Molecule Complexes

1. [NiNO(η^5-Cp)]

The first experimental study on the nature of the photoinduced change in [NiNO(η^5-Cp)] was by gas-phase EXAFS and gave evidence for a bending of the Ni−N−O angle to 160−133°. A subsequent photocrystallographic study of the pentamethylated compound (which unlike [NiNO(η^5-Cp)] is a solid at room temperature), performed at 25 K with 458 nm light, showed that the bond is indeed bent, but such as to give a side-bound (η^2) configuration, with a much smaller Ni−N−O angle of 92(1)°. As may be expected, the change is not completely confined to the NO ligand, as the pentamethylcyclopentadienyl ring is also distorted. While the Ni−Cp* distance does not change significantly, because on both Ni and Cp* move toward the NO position on isomerization, the methyl groups do not follow, presumably to preserve the van der Waals envelope of the molecule such as to maintain the intermolecular contacts. As a result, the C−CH$_3$ groups are bent out of the five-membered ring plane, as illustrated in Figure 8.[4] DFT calculations confirmed that the sideways bound species corresponds to a minimum on the potential energy surface, located at about 0.9 eV above the ground state. The DFT prediction of the existence of the second stable MS1-type state (η^1-O) of this nickel complex has recently been confirmed by IR spectroscopy. By using a 30 μm thin layer of the pure compound, sandwiched between two CsI disks, and irradiation at 77 K, Guida et al.[42] succeeded in observing the downshift typical for the MS1 type species. As is the case for SNP, on warming MS2 decays before MS1 (at 100−120 K, compared with 205−220 K for MS1), even though the former has the lower energy.

A new series of calculations on [Ni(NO)Cp] by Boulet et al.[43] generally reproduce the observed bond lengths in both the ground and metastable states,

Table 5. Decay Temperatures (K), GS NO Stretching Frequencies (cm^{-1}), and Observed Conversion Percentages for Several Ruthenium(II) Nitrosyl Complexes[a]

compound	MS1, T_d	MS2, T_d	ν(NO)	conversion[b] (%)	ref
$[Ru(bpy)(NO)(NO_2)(OH)(H_2O)][NO_2]$	193	no	1865	5	54
trans-$[Ru(NO)(OH)(py)_4][PF_6]_2$	223	no	1870	16	54
$K_2[Ru(NO_2)_4(NO)(OH)]$	208	173	1886	16/1	20
$K_2[RuCl_5(NO)]$	216	no	1895	5	46
trans-$[Ru(Br)(NO)(py)_4][PF_6]_2$	208	no	1902	7	54
trans-$[Ru(Cl)(NO)(py)_4][PF_6]_2 \cdot {}^1/_2H_2O$	256	171	1911	50/1	54
$[Ru(NH_3)_5(NO)][NO_3]_3$	265	no	1917	15	54
$[Ru(bpy)_2(NO)(H_2O)][ClO_4]_3$	231	188	1924	4/2	54
trans-$[Ru(NH_3)_4(NO)nic](SiF_6)(NO_3) \cdot H_2O$	250−260	no	1964, 1945	10	56

[b] Conversion percentage may not be maximal.

though, as for SNP, there is a basis-set and functional dependence of the theoretical results (Tables 1-3). As in SNP, the electronic structures of the GS and MS1 are quite similar, with the frontier orbitals having the same symmetry. The same is true for the transition states TSI and TSII. Further calculations[39] on the excited states of all three nitrosyl isomers shed light on the forward and backward photochemical processes. As for SNP, the excited state of [Ni(NO)Cp], which according to the DFT calculations results from the HOMO−LUMO $b_2 \rightarrow e$ transition, relaxes through a vibronic Renner−Teller distortion into a state with an NiNO angle very close to that of the GS/MS1 transition state on the ground-state potential curve. Its energy is only 0.13 eV above that of the transition state, thus leading to easy nonradiative relaxation into either the ground or the MS1 metastable state. From the MS2 state both forward and backward reactions are possible. The HOMO−LUMO transition leads to a configuration that is lower in energy than that of the MS2/MS1 transition state, so that this transition cannot lead to MS1. For the other excited states of MS2, either the NiNO angle is much smaller than that of the transition state or the states are quasi-dissociated, thus providing a logical explanation for the low yield of formation of MS1 of [Ni(NO)Cp]. Similar arguments show the MS2←MS1 photoreaction to be quite efficient. The nature of the excited states contrasts with that of SNP and related compounds, for which the MS2 has an excited state that can relax into a geometry beyond that of the MS2/MS1 transition state.

The original interpretation of the light-induced IR bands being due to a charge transfer from the Ni to the nitrosyl group is not confirmed by the theoretical calculations. While the HOMO−LUMO excitation corresponds to a charge transfer to the NO ligand, both the Hirshfeld and the Mulliken charge partitioning indicate only minor differences between the atomic charges of the GS, MS1 and MS2 states. The more consistent Hirshfeld analysis shows the variation on the Ni atom and the NO group upon rotation of NO to be at most 0.05 e.

It is of interest that several recent studies have found evidence for the existence of triatomic M−(η^2-NO) species. Zhou and Andrews[44] report that laser-ablated Fe, Co and Ni atoms react with NO to give side-bonded species during condensation in excess neon and argon. Similarly, Krim et al.[45] find that on co-condensation of Ni vapor and NO/Ar mixtures onto a cryogenic mirror at 10K both end-on and cyclic

Table 6. Decay Temperatures (K) and GS NO Stretching Frequencies (cm^{-1}) for Several Ru(II)(NO)(en) Complexes, As Measured by IR Spectroscopy[a]

compound	MS1, T_d	ν(NO)
trans-$[RuBr(NO)(en)_2]Br_2$	229	1877
trans-$[RuCl(NO)(en)_2]Cl_2$	246	1878
trans-$[Ru(H_2O)(NO)(en)_2]Cl_3$	267	1904
trans-$[Ru(Hox)(en)_2(NO)]Cl_2$	277	1900
cis-$[Ru(Hox)(ox)(en)(NO)]$	255	1888
cis-$[Ru(Hox)(en)_2(NO)]Cl_2 \cdot EtOH$	226	1917
cis-$K[Ru(ox)_2(en)(NO)]$	211	1881
cis-$[RuBr(en)_2(NO)]Br_2$	211	1881, 1902
cis-$[RuCl(en)_2(NO)]Cl_2$	206	1879, 1901

[a] From refs 49 and 55.

species, identified by IR spectroscopy and confirmed by theoretical calculations, are formed. Thus, it is likely that the linkage isomers of NiNO(η^5-Cp) are prototypes for a large family of related species.

2. Ruthenium and Osmium Complexes and the Dependence of the Decay Temperature on Chemical Substitution and S′

Not surprisingly, the photoinduced linkage isomerism is not limited to nitrosyl complexes of the first-row transition metals. The first Ru complexes for which long-lived metastable states were discovered are $K_2[RuCl_5NO]^{2-}$ [46] and $[Ru(NO_2)_4(OH)NO]^{2-}$,[47] which were followed by many others, including $[Ru(CN)_5NO]^{2-}$, the Ru analogue of the NP anion.[14]

Interestingly, for $[Ru(CN)_5NO]^{2-}$, and for the corresponding osmate, $[Os(CN)_5NO]^{2-}$,[48] the order of the decay temperatures is reversed, MS2 decaying at a higher temperature than MS1. For the osmate, the reported decay temperatures are 190 K for MS1 and 220 K for MS2. In the intermediate 190−220 K range, the spectral features due to MS1 decrease, but those for MS2 *increase*, indicating at least partial thermal conversion from MS1 to MS2. Obviously, the relative height of the MS1 → MS2 and MS2 → GS barriers depends on the size of the central atom, but also on the ligand, as for other Ru complexes which have been investigated the order of decay is "normal", i.e., as for SNP.

Decay temperatures and conversion percentages from DSC measurements and IR spectroscopy for a number of complexes are listed in Tables 5 and 6, respectively.[49] As described by Zöllner et al.,[8] the decay temperatures as measured by DSC are quite dependent on the heating rate applied in the experi-

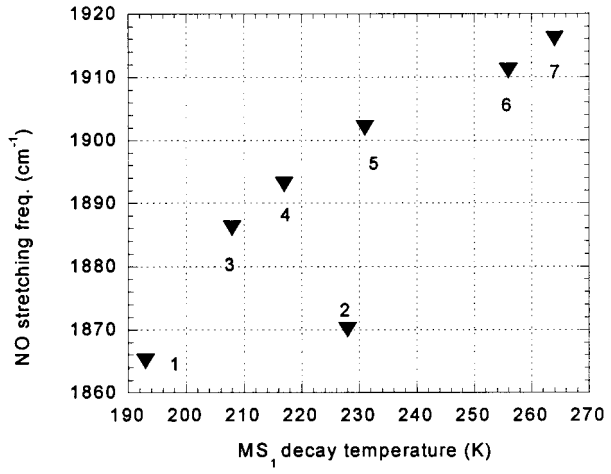

Figure 9. Decay temperature of MS1 (from DSC, 4 °C/min heating rate) as a function of the ground-state NO stretching frequency: (1) $[Ru(NO)(bpy)(NO_2)(OH)(H_2O)][NO_2]$, (2) $[Ru(NO)(OH)(py)_4][PF_6]_2$, (3) $K_2[Ru(NO)(NO_2)_4(OH)]$; (4) $K_2[Ru(NO)Cl_5]$; (5) $[Ru(NO)Br(py)_4][PF_6]_2$; (6) $[Ru(NO)Cl(py)_4][PF_6]_2$; (7) $[Ru(NO)(NH_3)_5][NO_3]_3$. (Reproduced with permission from ref 51. Copyright 1999 Gordon and Breach.)

ment, varying, for example, for SNP by about 20° when the rate is increased from 0.1 °C/min to 5 °C/min. Morioka et al.[21] define the decay temperature as the temperature at which the rate constant for the disappearance of the metastable species, as derived from the fading of the IR bands, is equal to 1×10^{-3} s^{-1}. This definition should lead to values lower than those based on the DSC curves, which are usually obtained at a temperature increase of 4−5 °C/minute. Thus, the decay temperatures in Tables 5 and 6 are not directly comparable. The highest decay temperature so far (277 K, from IR) is observed for *trans*-$[Ru(Hox)(en)_2NO]Cl_2$ (en = ethylenediamine, ox = oxalate).

The search for room-temperature stable NO-linkage isomers as high-capacity memory devices is of importance as high-capacity memory devices may be based on the change in refractive index that accompanies the transition.[50] It is thus of importance to examine dependence of the decay temperature be related on other physical properties. Can high T_d linkage isomers be designed?

The value of the decay temperature T_d of MS1 tends to correlate with the frequency of the ground-state stretching vibration of the NO group (as illustrated in Figure 9)[51] and with the suggested order of increasing π-donor ability $OH^- < NH_3 < Cl^- < SCN^- < Br^- < I^-$;[52] the NO bond getting weaker, the larger the π-donor ability of the trans ligand. OH^- appears to be an exception, which arguably can be explained on the basis of its σ-, rather than π-interaction.[53] No metastable state was found for $L = I^-$, which has an NO stretching frequency of 1832 cm^{-1}. Photochemical decomposition was observed in the case of $L = SCN^-$.[54] The data of Morioka and co-workers[49,55] on Ru nitrosyls with ethylenediamine as the cis ligand (Table 6) support for this hypothesis, as the same trend is found in this series with Br^-, Cl^-, and H_2O as trans ligands. Further examination of the entries of Table 6 shows that the nature of the equatorial ligand, though less important, cannot be discounted.

Though exceptions to the stretching frequency/decay temperature correlation occur, it suggests that a weak π-donor in the trans position with respect to NO stabilizes the L−Ru−ON fragment with the MS1 conformation. But the predictive value of the correlation is limited. In a subsequent study, Kim et al.[56] analyzed the $(SiF_6)(BF_4)$ and $(SiF_6)(NO_3)$ salts of *trans*-$[Ru(NH_3)_4(NO)nic]$, which have NO stretching bands at 1974 cm^{-1} (with a shoulder at 1918 cm^{-1}) and 1939 cm^{-1}, respectively, but found no increase in T_d, as DSC decay temperatures were observed in the 260−270 K range with both the IR and DSC techniques. It is possible, though by no means certain, that a limiting temperature is reached in the neighborhood of 0 °C.

The thermal stability of the linkage isomers depends on the energies of the transition states of the MS1 → MS2 and MS2 → GS processes, which apparently do not correlate precisely with the ground-state properties examined so far. The decrease in stability of the MS1 state with increasing π-donor ability of the trans ligand suggests a decrease in energy of the transition states on π-donation. Though the transition-state energies have been calculated with the linear transit method for several species (see for example Table 9), no successful optimization of the transition-state geometry, which would produce reliable energy barriers, has as yet been reported.

3. Solid-State Effects

The decay temperature of the salts of the nitroprusside (NP) ion depends moderately on the nature of the counterion.[57] Woike and co-workers investigated a large variety of salts of NP, including those of the first- and second-row metals Li−Cs and Be−Ba, the ammonium, tetramethylammonium, and acetamidinium ions, Zn, Tl, and Pb, Co, Ni, Cu, and Ag and others, most as single crystals, some as powers or cooled solutions in methanol or DMF or in a glassy matrix. Only MS1 was observed in the last two media. The decay temperatures reported vary from 132 to 151 K for MS2 and from 181 to 223 K for MS1. They report little difference between the MS1 decay temperature in crystalline solids and that in glassy matrixes and cooled solutions. The decay temperatures tend to be highest for divalent cations such as Tl^{2+} and Cu^{2+} and lower for the organic cations and in highly hydrated compounds. In agreement with this observation, and suggesting that larger dilution leads to lower decay temperatures, the MS1 decay temperature for the cocrystal of SNP with 18-crown-6, in which the effective cation is Na∈18-crown-6, has a decay temperature that is lower by 15° than that of SNP itself.[58] Differences between salts have also been observed for the Ru salts, with the nitrate of $[Ru(NH_3)_5(NO)]^{3+}$ having an MS1 decay temperature that is about 10° lower than that of the hexafluorophosphate salt.[58] The most unusual behavior is exhibited when $[Ru(NH_3)_5(NO)](NO_3)_3$ is absorbed in the pores of a silica gel glass. In the microporous solid the MS1 peak in the difference DSC (i.e., the dark-light curve) is downshifted by

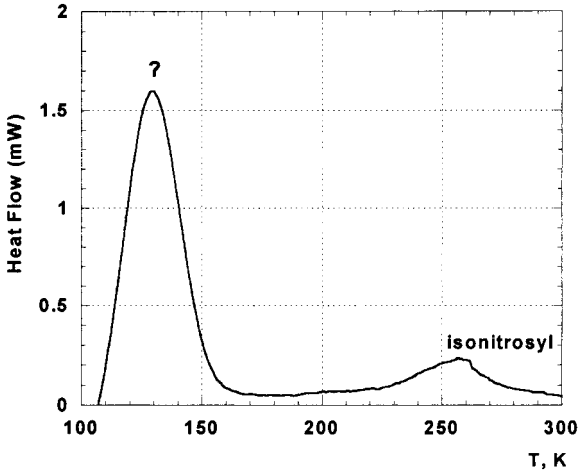

Figure 10. Difference DSC curve (dark-light) of $[Ru(NO)(NH_3)_5][NO_3]_3$ in a microporous silica gel glass. (Reproduced with permission from ref 58. Copyright 2000 Elsevier Science.)

about 10°, but with a greatly diminished intensity, while a pronounced new peak occurs at 130 K (Figure 10), which may correspond to an MS2-like species or an as yet unrecognized linkage isomer.[58]

It is likely that the decay temperatures in the condensed phases are affected by the size and shape of the reaction cavities. Though several definitions of the reaction cavity are possible, an often used definition is that of Ohashi et al.,[59] according to which walls of the cavity are defined by the neighboring atoms, each with a radius 1.2 Å larger than their van der Waals radius. Ohashi and co-workers[60] have argued that the 267 K decay temperature of the MS1 state of *trans*-$[Ru(H_2O)(NO)(en)_2]Cl_3$, which is high relative to that of SNP, is due to the shape of the reaction cavity. The NO cavity for this salt is tight for side-on coordination, thus increasing the barrier for deactivation, even though the volumes of the reaction cavities for this salt and SNP are very similar. Though electronic effects are likely to be dominant, there is undoubtedly a contribution of the matrix in condensed phases. An example is provided by the monoclinic crystals of $[NiNO(\eta^5\text{-Cp*})]$, which have two independent molecules in the asymmetric unit. Upon conversion to MS2, linkage isomers with a different orientation of the side-bound NO ligand with respect to the remainder of the molecule are formed. The orientation is clearly influenced by the shape of the reaction cavity, as illustrated in Figure 11.[58]

4. Theoretical Calculations on Ruthenium Complexes

In the first published theoretical calculations on the metastable states of Ru(NO) complexes Da Silva and Franco[61] conclude that the light-induced structures of $[Ru(NH_3)_5NO]^{3+}$ and $[Ru(NH_3)_4(OH)NO]^{2+}$ are consistent with a singlet excited-state structure stabilized by the geometry changes, as proposed earlier by Guida et al.[62] The argument is largely based on the observed shift of ν(NO) to lower frequency being incompatible with a putative decrease

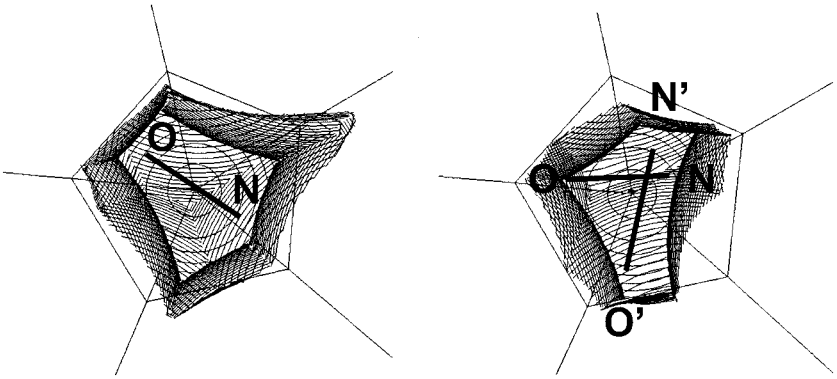

Figure 11. Reaction cavities for the two crystallographically independent molecules of $[Ni(NO)(\eta^5\text{-Cp*})]$ and the orientation of the NO ligand in the side-bound MS2 isomer, as determined experimentally: (a) molecule A, (b) molecule B. (Reproduced with permission from ref 58. Copyright 2000 Elsevier Science.)

Table 7. Effect of the Choice of Density Functional on the Geometry of the Ground State of the $[Ru(NH_3)_5(NO)]^{3+}$ Ion (Point Group C1)[a] (Bond Lengths in Å, Angles in deg)

	expt[b,c]	LDA	LDA relativistic	B88P86	B88P86 relativistic	BLYP	PW91
N−O	1.137(1)	1.131	1.134	1.131	1.142	1.128	1.138
$Ru-N_O$	1.785(21)	1.783	1.764	1.786	1.790	1.800	1.806
$Ru-NH_{3(trans)}$	2.094(9)	2.138	2.128	2.134	2.185	2.173	2.188
$Ru-NH_{3(eq)}$	2.101(2)	2.145	2.129	2.145	1.188	2.190	2.202
		2.142	2.129	2.145	2.186	2.195	2.198
		2.147	2.131	2.146	2.185	2.201	2.194
		2.147	2.131	2.145	2.186	2.195	2.198
∠Ru−N−O	179.2(3)	179.8	179.4	178.7	179.3	178.45	179.5
ν(NO), cm^{-1}	1917	2032	2023	2031	1953	2099	1971

[a] Reference 63. [b] Fomitchev, D. V.; Coppens, P. Unpublished results. [c] Standard deviations based on spread between three independent molecules.

Table 8. Selected Theoretical Results for the Ground States of [*trans*-LRu(NH$_3$)$_4$(NO)] Ions with Variable L (Experimental Values, When Available, Are Given in the Second Row of Each Entry)[a]

L =	OH^-	Cl^-	NO_2^-	H_2O	nic	NH_3
N−O (Å)	1.148	1.146	1.141	1.134	1.137	1.134
		1.142		1.144	1.136	1.139
ν(NO) (cm^{-1})	1955.7	1962.4	1979.1	2028.5	2001.2	2022.7
P_{NO} (e)[b]	0.0587	0.0658	0.0739	0.0747	0.0809	0.0839
∠N(O)−Ru−N (deg)	95.6	94.8	97.2	93.4	93.3	92.6
		92.1		93.7		93.1
ΔE(MS1) (eV)	1.945	1.918	1.803	1.948	1.790	1.822
T_d (K)	208[a]	216[b]			256[c]	260[d]

[a] Reference 58. [b] The π(NO) overlap population P_{NO}, defined as $P_{NO} = \sum_{\mu\nu} P_{\mu\nu} S_{\mu\nu}$ where the sum is over all π-orbitals on the two centers, $S_{\mu\nu}$ is the overlap integral between two basis functions ϕ_μ and ϕ_ν on the N and O atoms, respectively, and $P_{\mu\nu}$ are the products of their coefficients summed over all occupied spin−orbitals; P_{NO} increases on decreasing population of the antibonding orbitals. T_d = decay temperature of MS1: (a) for $K_2[Ru(NO)(NO_2)_4(OH)]$, (b) for $K_2[Ru(NO)Cl_5]$, (c) for both the $(SiF_6)(BF_4)$ and $(SiF_6)(NO_3)$ salts, (d) for the nitrate salt.

Table 9. Height of the Energy Barriers (eV) for $[Ru(NH_3)_5(NO)]^{3+}$, $[Ru(NH_3)_4Cl(NO)]^{2+}$, and $[Ru(NH_3)_4Br(NO)]^{2+}$ from the Linear Synchronous Transit Calculations[a]

	$[Ru(NH_3)_5(NO)]^{3+}$	$[Ru(NH_3)_4Cl(NO)]^{2+}$	$[Ru(NH_3)_4Br(NO)]^{2+}$
$\Delta E_I^{\ddagger}$ (GS→MS2)	1.171	0.722	0.566
$\Delta E_{II}^{\ddagger}$ (MS2→MS1)	0.562	0.460	0.239
T_d (K)	265[b]	256[c]	208[d]

[a] Reference 63. [b−d] Decay temperature T_d of MS1: (b) $[Ru(NO)(NH_3)_5][NO_3]_3$, (c) *trans*-$[RuCl(NO)(py)_4][PF_6]_2 \cdot {}^1/_2H_2O$, (d) *trans*-$[RuBr(NO)(py)_4][PF_6]_2$.

in d−π*ON mixing upon isonitrosyl formation and on the expectation of an ESR signal for a structure which could be described as consisting of Ru^{III} and ON^0. These results are at variance the X-ray structures of the metastable nitrosyl Ru complexes, including those of $K_2[Ru(NO)(NO_2)_4(OH)]$,[20] $[Ru(NO)(py)_4Cl][PF_6]_2$,[51,54] and *trans*-$[Ru(H_2O)(NO)(en)_2]Cl_3$,[60] and with subsequent theoretical calculations, which show that, as for SNP and $[NiNO(\eta^5\text{-Cp*})]$, the side-bound and isonitrosyl structures are diamagnetic species corresponding to local minima on the ground-state potential energy surface. However, subsequent DFT calculations of Ru complexes, summarized below, also fail to fully account for the softening of the NO stretching frequency of MS1 (but not of MS2) upon linkage isomer formation.

Novozhilova[63] calculated the $[Ru(NH_3)_5NO]^{3+}$ ion for a number of different functionals and found that very good agreement for the geometrical parameters of the grounds state is obtained with the LDA (local density approximation), using the VWN parametrization, including relativistic effects for the Ru atom (Table 7). The energy of MS1 is found to be 1.79 eV above that of the ground state. The fact that for SNP, with the same parametrization, a value of 1.746 eV is obtained, compared with a calorimetric value of 1.1 eV,[8,11] suggests that the theoretical result may be an overestimation of the energy difference. Frontier orbitals for $[Ru(NH_3)_5NO]^{3+}$ depicted in Figure 12 are in general agreement with DFT results for the nitrosyls of first-row transition metals discussed above. The qualitative similarity between the GS and MS1 orbitals is striking. The metal−NO binding in MS2 clearly has a significant contribution from the interaction between the NO-antibonding π* orbital and the metal d_{xz} orbital (orbital no. 30 in Figure 12; the *x*-axis is coplanar with the N−O bond).

To analyze the trans influence and obtain guidance for the synthesis of ligands with higher T_d, Kim et al.[56] reported a series of calculations on the ground states of *trans*-$Ru(NO)(NH_3)_4L$ complexes with varying trans substituent L. Selected results for the optimized geometries are summarized in Table 8, in which the high T_d *trans*-nic and *trans*-NH_3 complexes are listed on the right. The increase in NO stretching frequency toward the right of Table 8 is accompanied by a decreasing population of the NO antibonding orbitals, as may be expected. The geometric distortion expressed by the basal N(O)−Ru−N angle has been interpreted as a measure of trans influence.[64] However, it shows little systematic variation in the series. Though the theoretical MS1−GS energy differences are larger toward the left of Table 8, i.e., for the complexes with lower T_d values, no clear correlation is found. Further analysis will require precise calculation of the barrier heights for interconversion. Results for three complexes, given in Table 9, do indeed correlate with the values of the decay temperatures, but calculations on a larger series of compounds are clearly needed.

Quite extensive calculations, using the B3LYP hybrid functional and different basis sets, on the $[Ru(NH_3)_5(NO)]^{3+}$ and $[Ru(CN)_5(NO)]^{2-}$ ions by Gorelsky and Lever[65] reproduce known experimental geometries within hundredths of Å, and correctly predict the large softening of the NO stretching vibration on going from the ground state to MS2. The agreement with the IR data for MS1 is reasonable for $[Ru(NH_3)_5(NO)]^{3+}$, but quite basis-set dependent for $[Ru(CN)_5(NO)]^{2-}$, for which the larger DZVP basis set predicts no softening at all, whereas with the LANL2DZ set a softening of 50 cm^{-1} is obtained, compared with the experimental value of 100 cm^{-1}. Similar results are reported for the SNP anion. It is noticeable that the numerical basis set used by Delley et al.[33] for SNP also fails to reproduce the softening of the NO stretching frequency on MS1 formation.

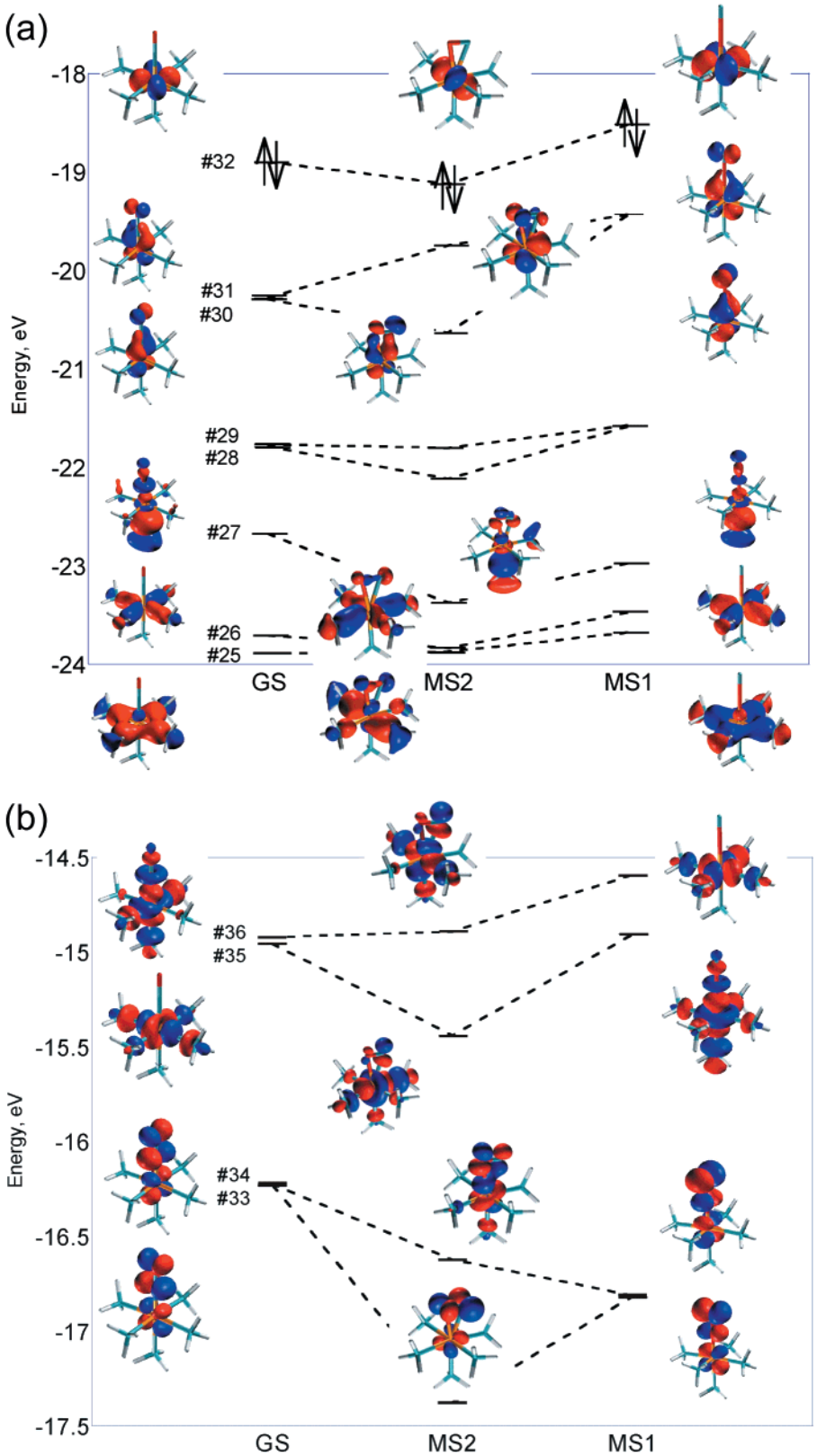

Figure 12. Calculated energy levels (in eV) and composition of selected molecular orbitals for the $[Ru(NH_3)_5(NO)]^{3+}$ complex: (a) bonding orbitals. The HOMO is indicated by an electron pair: (b) virtual orbitals. Orbitals were plotted with MOLDEN[128] using the adf2molden[129] conversion program.

While for SNP the calculations show that two isomers with eclipsed (MS2a) and staggered (MS2b) configurations are stable, in agreement with the work of Delley et al.,[33] it is found that for $[Ru(NH_3)_5(NO)]^{3+}$ and $[Ru(CN)_5(NO)]^{2-}$ the staggered configuration correspond to a transition state between the two eclipsed forms. However, in an independent DFT study on $[Ru(Cl)_5(NO)]^{2-}$ Novozhilova found both configurations to correspond to local minima.[35] As in the latter study a different program (ADF vs Gaussian98), different functionals (VWN vs B3LYP) and slightly different basis sets were used, a method-

Table 10. Structural Parameters of the Ground and Metastable States of the $[Ru(NH_3)_5(NO)]^{3+}$ Cation (Bond Lengths in Å, Angles in deg)

	GS				MS2			MS1		
	B3LYP LANL2DZ[a]	B3LYP DZVP[a]	VWN TZP[b]	expt[c,d]	B3LYP LANL2DZ[a]	B3LYP DZVP[a]	VWN TZP[b]	B3LYP LANL2DZ[a]	B3LYP DZVP[a]	VWN TZP[b]
N−O	1.166	1.129	1.134	1.137(1)	1.203	1.155	1.176	1.172	1.127	1.138
Ru−N_O	1.803	1.819	1.764	1.785(21)	2.043	2.045	1.931			
Ru−O_N					2.291	2.221	2.126	1.930	1.968	1.858
Ru−$NH_{3(trans)}$	2.176	2.194	2.128	2.094(9)	2.117	2.139	2.081	2.130	2.143	2.077
Ru−$NH_{3(eq)}$	2.198	2.211	2.130	2.101(2)	2.185, 2.228, 2.202, 2.202	2.203, 2.238, 2.214, 2.214	2.127, 2.148, 2.130, 2.130	2.199	2.213	2.128
∠Ru−N−O	178.8	179.3	179.4	179.2(3)	85.6	82.9	82.5			
∠Ru−O−N					62.8	66.0	64.2	179.2	179.3	179.7

[a] Reference 65. [b] Reference 63. [c] Fomitchev, D. V.; Coppens, P. Unpublished results. [d] Standard deviations are based on spread between three independent molecules.

Table 11. Comparison of Experimental and DFT-Calculated Hyperfine Parameters for the Ground and Metastable States of SNP in the Solid State and a Free Anion

parameter		expt	PWC[c] solid	PW91[c] solid	LAPW[d] solid	PWC-DND[c] free anion	LAPW[d] free anion
asymmetry, η	GS	0.021(8)[a]	0.08	0.04	0.03	0.00	0.10
	$MS2_{eclip/stag}$	<0.1[c]	*e*/0.40	*e*/0.44		0.94/0.30	0.51/*f*
	MS1	0.018(8)[a]	0.03	0.02		0.00	0.13
QS, mm/s	GS	1.716(3)[b]	1.78	1.55	1.71	1.60	1.31
	$MS2_{eclip/stag}$	2.862(3)[b]	*e*/3.08	*e*/2.81		2.12/2.95	2.48/*f*
	MS1	2.755(3)[b]	2.83	2.58		2.79	2.29
IS, mm/s	GS	0[b]	0	0		0	
	$MS2_{eclip/stag}$	0.194(3)[b]	*e*/0.17	*e*/0.17		0.15/0.16	
	MS1	0.178(3)[b]	0.11	0.12		0.13	

[a] Reference 68. [b] Reference 16. [c] Reference 33. Calculations carried out with double-numerical basis set with two *d*-polarization functions added on C, N, O; the basis set for Fe included a set of {3s3p3d4s4p} functions derived from Fe^{8+} ion. DND stands for double numerical basis set with one polarization function. [d] Reference 69. [e] Eclipsed conformation not stable in the solid state. [f] Values for staggered MS2 conformation not reported.

dependence of such results cannot be ruled out.

Gorelsky and Lever[65] explain the nonobservance of the MS2 state for the $[Ru(NH_3)_5(NO)]^{3+}$ complex by the absence of an excited state of MS1 with nonzero oscillator strength in the visible region. For $[Ru(CN)_5(NO)]^{2-}$ such a state exists, and MS2 has indeed been observed.

It is interesting that, while the NO distance is calculated to become longer by 0.03−0.04 Å on transition from GS to MS2, it is not generally predicted to be lengthened in MS1, notwithstanding the softening of the NO vibration. This is true for both SNP and the Ru complexes, and in agreement with the X-ray observations within the rather large standard deviations for this bond length. In $[Ru(NH_3)_5(NO)]^{3+}$, the calculations predict the metal to *trans*-ligand bond to be shortened from the GS geometry by 0.04−0.05 Å in both MS1 and MS2 (Table 10).

Two different conformations of the ligand trans to NO are possible in some of the complexes.[66] $[Ru(NH_3)_4L(NO)]^{3+}$ (L = H_2O, py, pyz) show two orientations of the L group: staggered or eclipsed conformations with respect to the equatorial ligands. According to the DFT calculations, the lowest energy structure for $[Ru(NH_3)_4L(NO)]^{3+}$ (L = py, pyz) corresponds to the staggered conformation of the L ligand, while for $[Ru(NH_3)_4(H_2O)NO]^{3+}$ the global energy minimum corresponds to the eclipsed geometry, the energy difference between the two being only 0.0054 eV.

Finally, we note that results on a series of B3LYP[67]/DZVP calculations of the electronic spectra of *trans*-$Ru(NO)(NH_3)_4L$ complexes correlate well with experimental results.[66]

5. Calculated Hyperfine Splittings and Comparison with Results from Mössbauer Spectroscopy

The quadrupole splittings (QS) and isomer shifts (IS) observed in the Mössbauer spectra on ^{57}Fe and ^{99}Ru isotopically labeled nitrosyl compounds provide a further opportunity to probe the nature of the nitrosyl linkage isomers.

Delley et al.,[33] as part of their theoretical study of SNP, found that the QS increases in the order GS → MS1 → MS2 for the molecule in the solid state (Table 11), in agreement with experiment,[16,68] while their free-ion calculations predicted the GS → MS2 → MS1 sequence. On the other hand, the free-ion LAPW calculations by Blaha et al.[69] predicted an ordering of the QS in agreement with the solid-state data. In both the solid state and free anion the isomer shift (IS) increases in the GS → MS1 → MS2 order, in agreement with experiment.[16,68] In all cases the MS2 asymmetry parameter is calculated to be much higher than observed experimentally (Table 11), a result attributed to the ease of rotation of the NO group around the symmetry axis of the remainder of the molecule.[69]

In the analogous ruthenium complex $[Ru(CN)_5NO]^{2-}$, the QS for the free anion in the ground state is calculated as +0.786 mm/s, in rather poor agreement with the experimental value of +0.49 mm/s.[70] The discrepancy was attributed to the uncertainty in the value of quadrupole moment Q of the excited

^{99}Ru nucleus and to the nonrelativistic approximation used in the calculation.

IV. Heme Systems

A. Introduction

As reviewed elsewhere[71] and discussed in other reviews in this issue, nitric oxide plays a crucial role in several important biological processes. Knowledge of the binding modes of nitric oxide (NO) to the heme group is thus essential to an overall understanding of the action of NO−heme-containing biomolecules. While much is known about the biological effects of NO, the detailed mechanism of NO uptake and release by the heme group remains to be fully elucidated. Kinetic studies of photochemically induced loss and recombination of NO with hemoproteins[72,73] and metalloporphyrins[74,75] suggest that recombination after photolysis is a fast and multistage process at room temperature.[76−78] The X-ray structure of nitrophorin 4, an NO−heme protein found in the saliva of the blood-sucking insect *Rhodnius prolixus*, has been interpreted as giving evidence for a loosely bound or side-on bound NO,[79] thus providing an impetus for more detailed studies on macromolecules. For such studies to be successful, detailed information on biologically relevant model compounds is essential.

B. Experimental Evidence for Linkage Isomers of NO Porphyrins and Theoretical Confirmation

Until recently, the established or proposed descriptions of NO binding to the metal center in heme or heme models were restricted to N binding of the NO group to the metal, either in the linear or the bent conformations. The first experimental evidence for the existence of alternative MS1-type NO-heme binding modes was provided by low-temperature (20 K) IR studies of (OEP)Ru(NO)L (OEP = octaethylporphyrin) with L = O-*i*-C_5H_{11}, SCH_2CF_3, Cl, and py, which all have the {MNO}^{6} electronic configuration.[80] The experimental evidence, obtained on samples in KBr, can be summarized as follows:

(1) Photolysis does not produce free NO, as the 1880 cm^{-1} absorption band typical for free NO is absent.[81]

(2) The parent nitrosyl bands are restored on subsequent warming, and their full intensity is recovered on subsequent cooling back to 20 K. In all cases, the photoinduced bands persist for at least several hours if the initial temperature is maintained.

(3) The new bands are subject to the ^{15}N-isotope shift and thus associated with ν(NO).

(4) The observed decreases of ν(NO) upon conversion from nitrosyl to isonitrosyl (η^1-O) and to side-on (η^2-NO) bound nitrosyl are very similar to those recorded for the excited Fe, Ru, Os and Ni nitrosyl complexes described earlier in this review.[6,14,20,46,64]

(5) Downshifts of a number of porphyrin skeletal modes (in the 1600−900 cm^{-1} region)[82,83] by 3−5 cm^{-1} upon photolysis are consistent with the data available for six-coordinate Fe(II) porphyrins, which indicate that the reduction of the π-acid character of the axial ligand causes downshifts of the skeletal absorption bands.[84]

A subsequent study of several five-coordinate Fe porphyrins, with the {MNO}^{7} configuration, was accompanied by DFT calculations on both the ground state and the photoinduced linkage isomers.[85] For the complexes Fe(TTP)NO (TTP = tetratoluylporphyrin) and Fe(OEP)NO, irradiation of KBr pellets at 25 K results in the formation of new MS1-type bands in the IR spectra, again downshifted from the parent NO stretching frequencies. The spectral changes for the $^{14}N^{16}O$, $^{15}N^{16}O$, and $^{15}N^{18}O$ complexes of Fe(OEP) and Fe(TTP) are illustrated in Figure 13. As for the Ru analogues, subsequent warming results in the disappearance of all new bands and the restoration of the original spectra.

Parallel DFT calculations with the local density approximation (LDA) were performed on FeP′(NO) (P′ = porphine dianion).[63] The ground-state optimization of FeP′(NO) reproduces the structural distortions observed by Ellison and Scheidt for Fe(OEP)(NO).[86,87] As observed by X-ray diffraction, the Fe−N(O) vector is tilted away from the normal to the plane through the four equatorial N atoms toward the oxygen atom (by 8° according to the optimization, 6−8° according to experiment), while the NO group is staggered with respect to the equatorial bonds. The four equatorial Fe−N distances divide in two groups with the bonds closest to the direction of the NO tilt being shorter by ∼0.025 Å, as observed generally in {FeNO}^{7} complexes and interpreted by Scheidt and Ellison in terms of increased d_{z^2}-NO π* interaction with rotation of the d_{z^2} orbital away from the plane normal, and accompanying tilting of the basal σ-orbitals, leading to a stronger Fe−N(por) interaction in the direction of the tilt.[88]

The orientation and symmetry of the π*(NO) orbitals with respect to the metal orbitals are schematically depicted in Figure 14a.[63] The p_x and p_y orbitals on the proximal atom of the NO ligand overlap in phase with the metal d_{xz}, d_{yz} atomic orbitals, respectively. Parts b and c of Figure 14 show the resulting HOMO-2 and HOMO-3 metal−NO bonding orbitals, while the singly occupied HOMO, which is antibonding in the metal−ligand region, is shown in Figure 14d.

Optimization of the staggered MS1 isonitrosyl structure FeP′(ON) confirms that it corresponds to a local energy minimum with an energy 1.59 eV above that of the ground state. Unlike in SNP,[33] neither the eclipsed isonitrosyl configuration for FeP′(ON) nor the η^2 side-on MS2 geometry were found to correspond to local minima, in agreement with the absence of corresponding features in the IR spectra. The theoretical geometry of the MS1 state of the complex is depicted in Figure 15.

C. Further Theoretical Studies on NO-Porphyrins

Using density functional theory (PW91 functional), Wondimagegn and Ghosh[89,90] performed a comprehensive search for stable metastable states in a number of nitrosylmetalloporphyrin complexes with {MNO}^{n} (n = 6−8) configurations, where M = Mn,

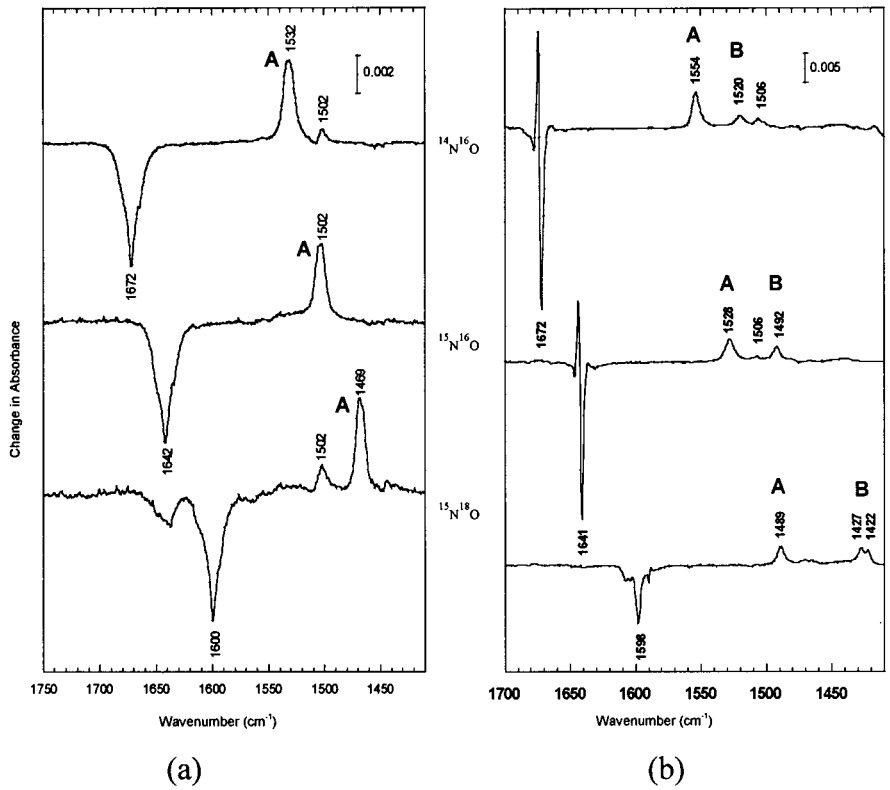

Figure 13. Infrared difference spectra obtained by subtracting the spectra of the complex after illumination (at 25 K) from the infrared spectra of the complex in the dark, for different isotopic substitutions: (a) Fe(TTP)(NO), (b) Fe(OEP)(NO). Negative and positive features represent IR bands that are depleted or new/increased in intensity upon illumination, respectively. The differential feature of the highest frequency band of Fe(OEP)(NO) is due to a slight change in peak profile. (Reproduced with permission from ref 85. Copyright 2000 The American Chemical Society.)

Fe, Co, Ru, Rh. In all species examined the isonitrosyl MS1 isomer corresponds to a local minimum on the ground-state potential energy surface. The isonitrosyl isomers were found to be 1.20−1.47 eV higher in energy than the corresponding ground state. The η^2 side-bound configuration is found to be stable only in certain cases, including MnP(NO), $FeP(NO)^+$, RuP(NO)Cl, and $[Ru(NO)Cl]^+$, but unlike in other studies, at an energy higher, rather than lower, than the η^1-NO isomer. The metastable side-bound isomers predicted in this study all have the $\{MNO\}^6$ configuration, though it may be noted that the existence of a metastable η^2 isomer is firmly established both theoretically and experimentally for the $\{MNO\}^{10}$-configuration complex [Ni(NO)Cp], as described in Section III.C.1.

The authors report that in many other cases, especially with axial substitution, attempts to optimize the side-bound isomer of the $\{FeNO\}^6$ species led to an η^1 geometry with a strongly bent Fe−N−O angle, but with a longer, nonbonded Fe−O distance than is the case for η^2. This structure has not been observed in high-resolution X-ray studies, although it resembles one of the conformers recently reported for nitrophorin 4, based on a 1.4−1.6 Å resolution structure determination.[79]

V. Linkage Isomerism of Other Di- and Triatomic Ligand Transition-Metal Complexes

A. Dinitrogen

Molecular nitrogen is a simple and relatively inert molecule. Its ability to bind to transition metals has only been known since 1965 when Allen and Senoff discovered the $[Ru(NH_3)_5(N_2)]^{2+}$ ion.[91] An early claim of the observation of the alternate η^2 (side-on) binding mode of N_2 to a single metal atom in a ground-state structure[92] was not confirmed by a more detailed analysis.[93] In 1970, Armor and Taube[94] showed, using IR spectroscopy, that isotopically labeled $[Ru(NH_3)_5(^{15}NN)]^{2+}$ in time converts to a mixture of the parent ion and $[Ru(NH_3)_5(N^{15}N)]^{2+}$, suggesting end-to-end rotation of N_2 through the side-on bound state of N_2.

Further IR evidence indicated its existence, either as an intermediate or as a stable configuration in inert matrixes or on surfaces. Ozin and Vander Voet[95] found a single IR absorption band for the $Co^{14}N^{15}N$ species isolated in a dilute nitrogen−argon matrix at 10 K, a clear indication of side-on binding for this species, in contrast to the Fe and Ni analogues, for which the $^{14}N^{15}N$ band is split into two lines of equal intensity. Similar evidence was subsequently obtained in other studies.[96] Side-bound N_2 is also found on catalytic Fe and Ru surfaces,[97] prior to N_2 dissociation and ammonium synthesis.

The widespread occurrence of photoinduced linkage isomerism in group 8 transition-metal nitrosyl complexes, and the above-summarized evidence for N_2, was the motivation for a photocrystallographic study of $[Os(NH_3)_5(N_2)](PF_6)_2$ salt by Fomitchev et al.[98] The formation of a new species upon irradiation is evident both by IR and by DSC. Analogous to the nitrosyl compounds, a new 1838 cm^{-1} IR band, downshifted by 187 cm^{-1} from the parent band at 2025 cm^{-1}, is generated at 1838 cm^{-1} upon irradiation with a Xe

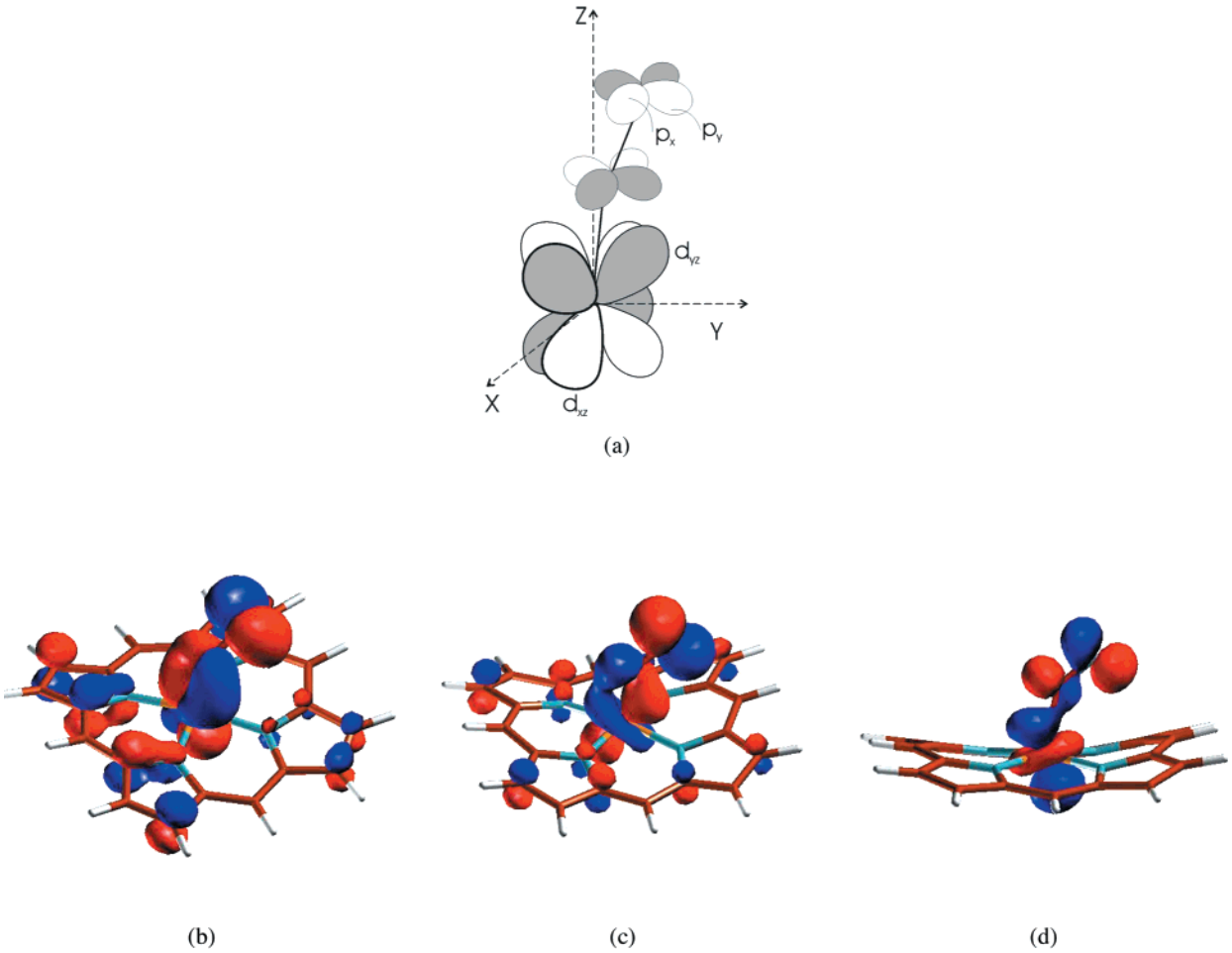

Figure 14. Molecular orbitals relevant to {FeNO}^{7} tilting in MS1 of FeP′(NO): (a) schematic illustration of $d_{(xz,yz)}-p_{(x,y)}$-(NO) π-interaction and corresponding bonding molecular orbitals (b) no. 67 (SOMO-3) and (c) no. 68 (SOMO-2). The molecular orbitals shown have equal contributions from the d_{xz} and d_{yz} metal orbitals, no. 68 also has a d_{z^2} contribution; (d) $d_{z^2}-\pi^*$-(NO) interaction in half-occupied molecular orbital no. 70 (SOMO).

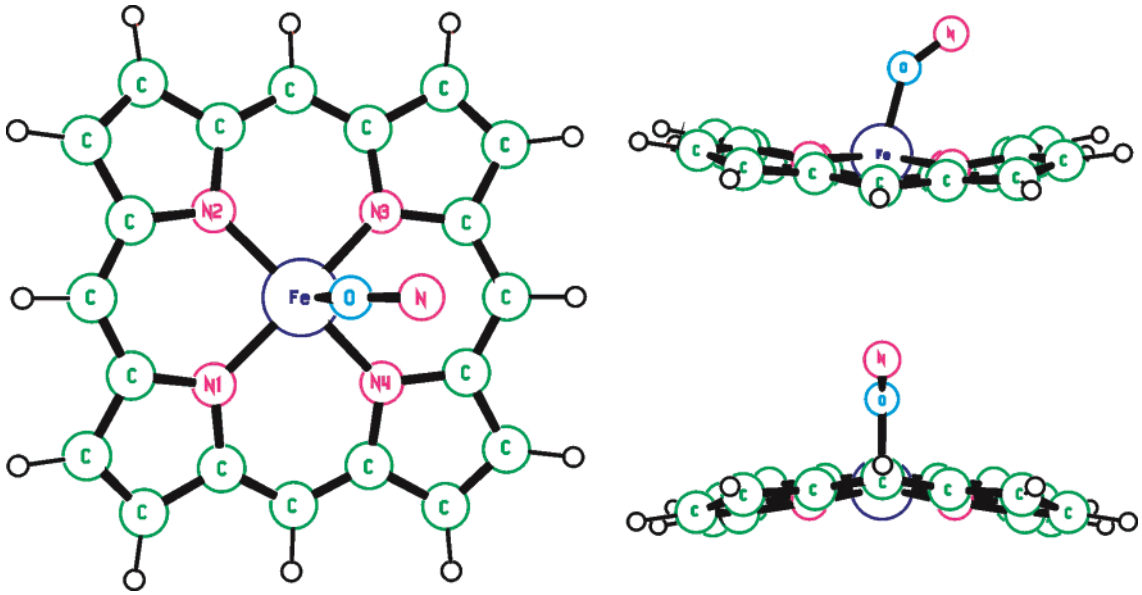

Figure 15. Theoretical geometry of the MS1 state of FeP′(ON). (Reproduced with permission from ref 85. Copyright 2000 The American Chemical Society.)

lamp ($330 < \lambda < 460$ nm) at 100 K. As for the nitrosyl compounds, the light-induced band disappears and the intensity of the original stretch of (η^1) N_2 is restored when the light is switched off and the sample warmed to room temperature. DSC of an irradiated sample shows a decay temperature of

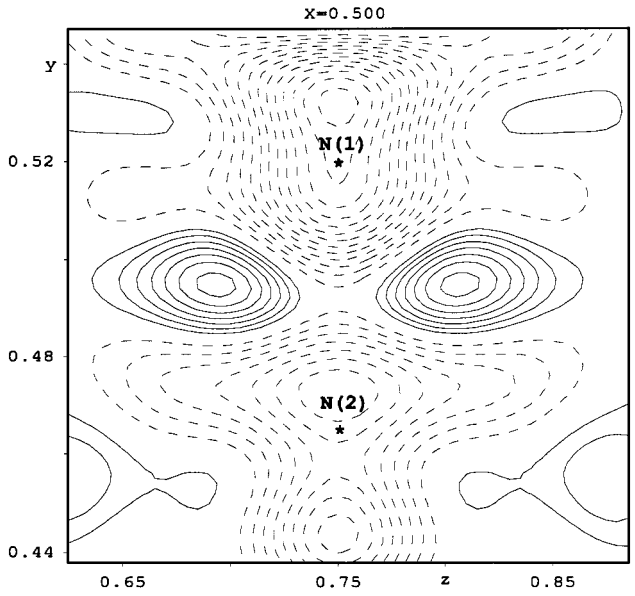

Figure 16. Crystallographic photodifference map of $[Os(NH_3)_5(N_2)](PF_6)_2$. Difference between the electron density in the excited crystal and the ground-state density in a plane containing the N_2 ligand. The change in orientation of the ligand is manifested by electron-deficient regions (broken lines) around the original positions of the nitrogen atoms and two new peaks (solid lines) at the atomic positions of the light-induced side-on bound ligand. Contour interval 0.2 e/Å^3.

Table 12. Structural Parameters of the GS and MS1 States of $[Os(NH_3)_5(N_2)]^{2-}$ [a,b]

	GS	MS2
Os−N(1)	1.848(2)	2.109(16)
	1.877	2.142
N(1)−N(2)[c]	1.128(3)	1.07(3)
	1.122	1.142
$Os-N_{eq}$	2.1348(1)	2.169(8)
	2.074	2.077
$Os-N_{ax}$	2.151(3)	2.108(14)
	2.073	2.038
∠N(2)−N(1)−Os	180.0	75.3(4)
	180.0	74.64
$\angle N(1)-Os-N_{ax}$	180.0	165.3(4)
	180.0	164.69
$\angle N_{eq}-Os-N_{ax}$	89.10(3)	80.5(3)
	91.7	87.63

[a] First entry: experiment. Second entry: DF theory (B88P86/VWN, STO triple-ζ basis set with a polarization function added on N and H atoms) (bond lengths in Å, angles in deg). [b] N(1) and N(2) are the atoms of the dinitrogen ligand. [c] N(1) and N(2) are related by symmetry in the side-bound structure.

about 218 K. The crystallographic photodifference map indicates the existence of a side-bound species (Figure 16), which is confirmed by both least-squares refinement and DFT calculations.

The agreement between the experimental and theoretical geometries is quite reasonable, as shown in Table 12. As the molecule is located on a site of C_{2v} symmetry, the side-bound dinitrogen ligand occurs in two orientations. Combined with the presence of the heavy Os atom, this leads to low accuracy in the experimental N−N bond length of the MS2 state. Other geometry changes, such as the shortening of the axial trans bond and the decrease in the $X_{eq}-M-X_{ax}$ "umbrella" angle, are as observed for the MS2 nitrosyl linkage isomers. The theoretical values reproduce these changes and predict a slight lengthening of the N−N bond.

Though the above study is the only example so far of a light-induced side-on metastable state of dinitrogen, there are likely many as yet undetected examples. It is quite possible that side-bound dinitrogen also plays a role in biological nitrogen fixation mediated by the nitrogenase enzyme, as it does in catalyzed industrial processes on metal surfaces.

B. NO_2

The ambidentate nature of the nitro group has been known for more than a century. In 1898, Jørgensen[99] synthesized Co(III)ammine(NO_2) complexes and found that nitrito, ONO, isomers not only can be synthesized directly in solution but also are formed upon irradiation of the corresponding solid NO_2 isomers. Jørgensen concluded that the isomerization proceeds intramolecularly.

The first detailed study on the photochemical behavior of NO_2-containing transition-metal complexes was done by Adell in 1955,[100] who showed that the red compound obtained from $[Co(NH_3)_5NO_2]Cl_2$ on prolonged exposure to sunlight is the O-bound nitrito isomer, formed according to the reaction

$$Co(NH_3)_5NO_2^{2+} \xrightarrow{h\nu} Co(NH_3)_5ONO^{2+}$$

This result was subsequently confirmed by Wendlandt and Woodlock,[101] who initiated the reaction by UV irradiation. Further extensive studies were done by Balzani and co-workers.[102] Solid-state irradiation at room temperature with 254, 343, 365, and 442 nm light showed a progressive decrease in intensity of the infrared bands at 1430, 1315, and 825 cm^{-1} (N-bound nitrite), while new bands at 1460 and 1065 cm^{-1} were attributed to O-bound nitrite. Using Nujol mulls as IR samples, the authors could obtain almost complete conversion of the nitro into the nitrito form. However, the nitrito isomers are not thermodynamically stable. When irradiated samples are placed in the dark at room temperature, a back-reaction takes place with the final IR spectrum being identical to that of the original complex.

Grenthe and Nordin[103] compared the chemically synthesized chloride of $[Co(NH_3)_5ONO]^{2+}$ with samples obtained by irradiation of the corresponding nitro linkage isomer with a tungsten lamp. Powder diffraction patterns indicated that both the thermal nitrito → nitro and the reverse photoreaction proceed with retention of crystallinity, but the diffraction pattern of the photoisomerisation product is different from that of the chemically synthesized crystals. The thermal reaction was found to be a two-step process, believed to proceed through a seven-coordinate transition state, though, given the current insight, a bidentate intermediate provides an alternative explanation.

The same authors studied the iodide and perchlorate salts of *trans*-$[Co(III)(en)_2(NCS)(NO_2)]^{2+}$.[104] Upon irradiation, the perchlorate yields the nitrito form with 80% yield, the reaction again proceeding with retention of crystallinity. In this case, the photoproduct and the original nitrito compound gave identical

diffraction patterns. The as-synthesized nitrito complex was found to have a half-life of 320 h at room temperature and thus is much more stable than any of the isonitrosyl complexes currently known.

In a subsequent study, Heyns and Waal[105] compared the IR spectra of the photochemically and synthetically prepared nitrito form of $[Co(NH_3)_5NO_2]Cl_2$ and found that freshly prepared $[Co(NH_3)_5(ONO)]Cl_2$ shows sharper and better-defined IR absorption peaks, indicating that the sample prepared by chemical methods has a more ordered structure than that obtained by photochemically. Two new bands at 1460 and 1055 cm^{-1} appear upon irradiation but disappear after the sample is stored in the dark for several days.

Two X-ray crystallographic studies on the geometry of the species induced on photoisomerization of $[Co(NH_3)_5NO_2]^{2+}$ have been reported. In a low-temperature single-crystal study of the nitrito form, Kubota and Ohba[106] irradiated the nitro compound with unfiltered light from a 150 W Xe lamp. The O-bound NO_2^- was found to be bent, with a Co−O−N bond angle of 143(4)°. The population of $[Co(NH_3)_5ONO]^{2+}$ refined to approximately 15%. In this study, only the atoms of the ONO ligand of the photoinduced species were refined, a possible reorientation or change in geometry of the remainder of the molecule was not considered, and might have been difficult to detect, given the conversion percentage and the occurrence of two alternate orientations of the nitrito group.

In a second study, Masciocchi and co-workers[107] chose the $[Co(NH_3)_5NO_2]Br_2$ salt rather than the chloride for an X-ray powder diffraction study. They used direct sunlight rather than an artificial light source and reportedly achieved a 100% yield of the nitrito isomer. In contrast to the results of the single crystal study, they concluded that the Co−O−N fragment is linear. However, the single-crystal results on the chloride are likely to be more reliable.

It is remarkable that the first indication of a photoinduced η^2 bonding mode of the N−O moiety was made in 1975, before the discoveries of photoinduced nitrosyl species, and long before their identification. Johnson and Pashman[108] performed low-temperature IR experiments (at 77 K) on a crystalline sample of $[Co(NH_3)_5NO_2]Cl_2$ and found a new transient IR band at 1110 cm^{-1}, accompanied by a bleaching of bands associated with the N-bound species, an observation interpreted by the formation of a bidentate ligand:

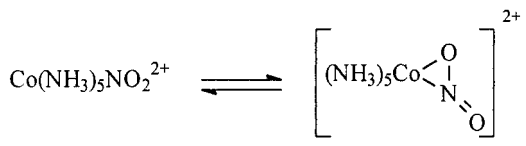

On warming, the 1110 cm^{-1} band disappears and a new band at 1050 cm^{-1} typical for the nitrito isomer occurs in parallel with the bleaching of the1110 cm^{-1} band. This process has not been investigated further but is very likely analogous to that now confirmed for the transition-metal nitrosyl complexes.

Matrix isolation studies at 13 K on photolysis of $CpRu(CO)_2NO_2$ using FTIR have provided information on a series of new reaction products, with various lifetimes and coordinations of the nitro group.[109] The proposed matrix photochemistry of $CpRu(CO)_2NO_2$ is summarized in Scheme 1. Experiments on single crystals would be valuable for further identification of the proposed species.

The photochemistry of $[Co(NH_3)_5NO_2]^{2+}$ and other nitro-containing transition-metal complexes has also been studied in solution. Three distinct photochemical processes occur on irradiation: (i) nitro−nitrito linkage isomerization; (ii) NO_2 solvatation; and (iii) oxidation or reduction, resulting in complete destruction of the corresponding complex.[110−114]

C. Sulfur-Containing Ligands

SO_2 is an ambidentate ligand, isoelectronic with NO_2^-, and capable of binding in several different ways to a metal center (i−vi), as illustrated below (Scheme 2).

In the first reported solid-state photochemical study of transition-metal complexes with sulfur-containing ligands, Johnson and Dew in 1979[115] recorded the low-temperature IR spectra of irradiated *trans*-$[Ru^{II}(NH_3)_4(SO_2)Cl]Cl$. Irradiation of both KBr pellets and Nujol mulls at 195 K with 365 nm light produced two new IR bands at 1165 and 940 cm^{-1}, compared to 1255 and 1110 cm^{-1} in the starting complex. ^{18}O isotopic substitution gave strong evidence for formation of the η^2-S,O-bound SO_2 isomer (iii). Photolysis at the lower temperature of 25 K for only 30 s to 2 min produces an additional feature at 1180 cm^{-1}, indicating a second light-induced species. Prolonged photolysis at 25 K, or cooling of the 195 K irradiated sample to 25 K and subsequent photolysis, produces a third species, identified by IR bands at 1285, 1130, and 560 cm^{-1}. However, the IR results did not allow the authors to identify the possible structures of the second and third isomers, though they note that the spectral features are not inconsistent with the pyramidal structure ii for the short irradiation species and the O-bound isomer iv or v for the species obtained after prolonged 25 K irradiation.

Very recent photocrystallographic results by Kovalevsky et al.[116] confirm the formation of the η^2-S,O-bound SO_2 isomer upon irradiation with either 355 or 488 nm light and give information on its geometry. DSC measurements show the species to decay at 257 K on warming, while a second, as yet unidentified species obtained on low-temperature irradiation with 355 nm light decays at 170 K.

Upon irradiation with white light of the $[Co(pyse)(en)_2](ClO_4)_2$ complex (pyse = 2-pyridinesulfenate (1−)) in the solid state, its color changes from orange to green. XPS spectra of both compounds suggested the following linkage isomerization:[117,118]

The green complex is quite stable, with a decay temperature much higher than 293 K. However, the corresponding sulfinato complex (with two oxygen atoms bonded to S) was unstable and easily linkage-isomerized either photochemically or thermally to the orange pysi (pysi = 2-pyridinesulfinate (1−)) N,O complex.

Like the cyano group, the thiocyanate ion forms either thiocyanate (M-*S*CN) or isothiocyanate (M-

Scheme 1

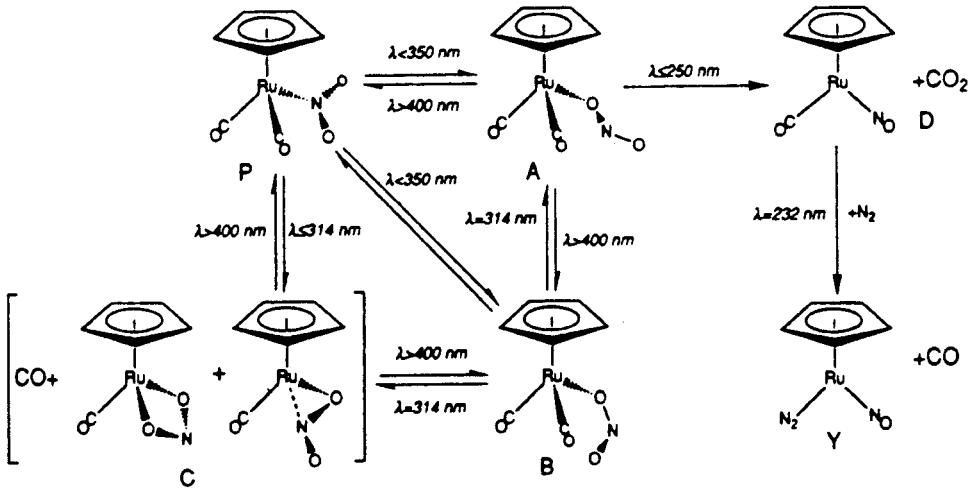

Scheme 2

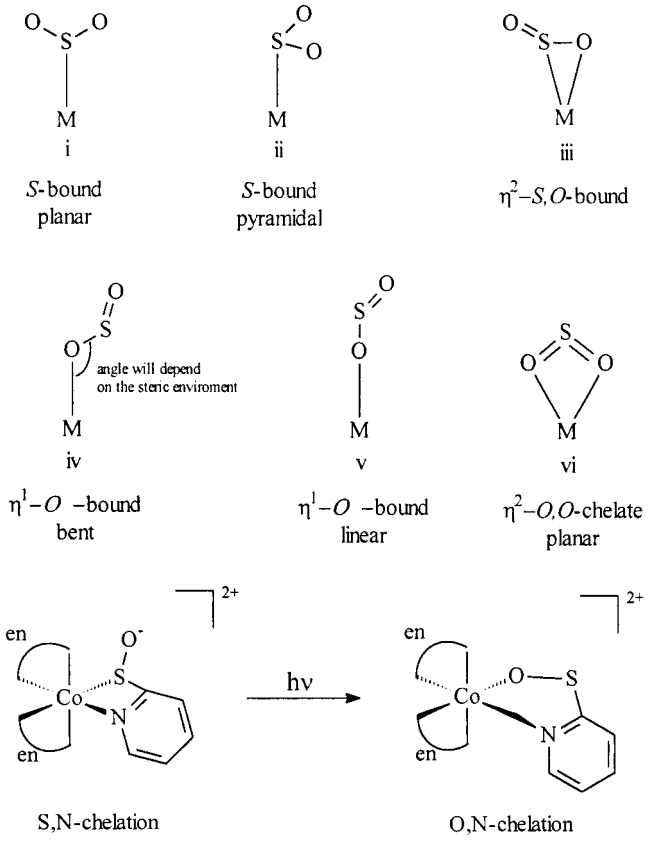

*N*CS) metal complexes depending on the nature of the metal and of other ligands attached to the metal atom.[119] The N- to S-bound linkage isomerization can be achieved thermally in the crystalline phase.[120] A γ-ray induced (^{57}Co source) N- to S-bound isomerization of tetrahedrally coordinated $M_2[Fe(NCS)_4]$ ($M = Me_4N^+$, Et_4N^+, K^+) complexes was reported by Wei and Ho.[121] Two sets of quadrupole-split doublets in both absorption and emission Mössbauer spectra were observed, consistent with the existence of S-bound thiocyanates in the irradiated compound. The proposed linkage isomerism was supported by comparison of the IR spectra of nonirradiated and γ-irradiated samples.

Linkage isomerization of the DMSO complex $[Ru(bpy)_2(DMSO)_2](PF_6)_2$ can be induced by sunlight and is reported to be completely reversible.[122] The yellow to red color change reverts in the dark and is explained by an S-bound to O-bound isomerization taking place in DMSO and DMSO/nitromethane solutions.

DMSO, though larger than the other small ligands discussed here, can reorient in the solid state. An immediate color change from yellow to red was observed upon irradiation of a crystalline sample of $[Ru^{II}(trpy)(bpy)(DMSO)](SO_3CF_3)_2$ with 441.6 nm light at room temperature.[123] The original color returned only after several minutes. The red species has a weak luminescence band at 720 nm, which is attributed to an *O*-bound Ru-DMS*O* photoproduct. At lower temperatures a new luminescence band at 625 nm appears, which is assumed to be due to η^2-coordinated DMSO.

Extensive studies on the solution photochemical behavior of transition-metal complexes with sulfur-containing ligands have been reported.[124−127] Unlike the nitro-complexes, the photoproducts do not decompose upon irradiation and are often thermally stable. Several have been isolated as pure compounds.

VI. Concluding Remarks

More than 20 years after the discovery of novel features introduced upon light-irradiation of nitrosyl compounds and 6 years since their identification as linkage isomers, it is apparent that photoinduced linkage isomerism of di- and triatomic molecules bonded to transition-metal atoms is a quite common phenomenon. Many of the new species decay close to ambient temperatures, and thus, though transient, will have relatively long lifetimes at physiological temperatures. Their role in the kinetics of biological processes remains to be elucidated. The new species may have unusual reactivity, which merits further attention.

VII. Acknowledgments

Financial support by the National Science Foundation (CHE9981864) and the Petroleum Research Fund of the American Chemical Society

(PRF32638AC3) is gratefully acknowledged. The Center for Computational Research of the State University of New York at Buffalo is supported by a grant (DBI9871132) from the National Science Foundation.

VIII. Abbreviations

ADF	Amsterdam density functional program
B3LYP	Becke (1993) three-parameter hybrid density functional using Lee, Yang, and Parr (1988) correlation functional
BLYP	Becke (1988) and Lee, Yang, and Parr (1988) gradient-corrected density functional
B88P86	Becke (1988) and Perdew (1986) gradient-corrected density functional
bpy	2,2′-bipyridyl
CI	configuration interaction
CISD	CI with all single and double substitutions
Cp	cyclopentadienyl ligand
Cp*	pentamethyl cyclopentadienyl ligand
CT	charge transfer
DFT	density functional theory
DMF	*N*,*N*-dimethylformamide
DMSO	dimethyl sulfoxide
DND	double numerical basis set with a polarization function
DSC	differential scanning calorimetry
DZVP	double-ζ valence basis set with a polarization function
en	1,2-ethylenediamine
ESR	electron spin resonance
EXAFS	edge X-ray absorption fine structure
FTIR	Fourier transform infrared spectroscopy
HF	Hartree−Fock, an ab initio self-consistent field method
HOMO	highest occupied molecular orbital
GGA	generalized gradient approximation
GS	ground state
GTO	Gaussian-type basis functions
INDO	intermediate neglect of differential overlap
IR	infrared spectroscopy
LANL2DZ	Los Alamos National Laboratory double-ζ pseudo-potential basis set
LAPW	full-potential linearized augmented plane wave method for crystal-property calculations
LDA	local density approximation
LUMO	lowest unoccupied molecular orbital
MS1	oxygen-bound (η^1-O) nitrosyl, i.e., isonitrosyl
MS2a	side-on (η^2-NO) bound nitrosyl; NO ligand is eclipsed with respect to the equatorial ligands
MS2b	side-on (η^2-NO) bound nitrosyl; NO ligand is staggered with respect to the equatorial ligands
nic	nicotinamide
ox	oxalate
NP	nitroprusside
OEP	octaethylporphyrin
P′	porphine dianion
PW91	Perdew and Wang (1991) gradient-corrected density functional
PWC	Perdew and Wang (1992) local-density functional
py	pyridine
pyse	2-pyridinesulfenate(1−) ion
SCCC-MO	self-consistent charge and configuration molecular-orbital method
SINDO	symmetrically orthogonalized intermediate neglect of differential overlap
SNP	sodium nitroprusside
STO	Slater-type basis functions
T_d	decay temperature
trpy	2,2′;6′,2″-terpyridine
TTP	tetratoluylporphyrin
TZP	triple-ζ STO basis set with a polarization function
VWN	Vosko, Wilk, and Nusair (1980) local density functional
XANES	X-ray absorption near-edge structure
XPS	X-ray photoelectron spectroscopy

IX. Note Added after ASAP Posting

In section IV.C the sentence "The η^2 side-bound configuration is found to be stable only in certain cases, including MnP(NO), $FeP(NO)^+$, RuP(NO)Cl, and $[Ru(NO)Cl]^+$, but unlike in other studies, at an energy higher, rather than lower than the η^1-NO isomer" should read as follows: The η^2 side-bound configuration is found to be stable only in certain cases, including MnP(NO), $FeP(NO)^+$, RuP(NO)Cl, and $[Ru(NO)Cl]^+$, as in other studies, at an energy higher than the η^1-NO species.

X. References

(1) (a) Cohen, M. D.; Schmidt, G. M. J. *J. Chem. Soc.* **1964**, 1996. (b) Cohen, M. D. *Angew. Chem.* **1975**, *14*, 386.
(2) Coppens, P. *Synchr. Rad. News* **1997**, *10*, 26.
(3) Fullagar, W. K.; Wu, G.; Ribaud, L.; Kim, C. D.; Sagerman, G.; Coppens, P. *J. Synchr. Rad.* **2000**, *7*, 229.
(4) Fomitchev, D. V.; Furlani, T. R.; Coppens, P. *Inorg. Chem.* **1998**, *37*, 1519.
(5) (a) Carducci, M. D.; Pressprich, M. R.; Coppens, P. *J. Am. Chem. Soc.* **1997**, *119*, 2669. (b) Coppens, P.; Fomitchev, D. V.; Carducci, M. D.; Culp, K. *J. Chem. Soc., Dalton Trans.* **1998**, 865.
(6) Crichton, O.; Rest, A. J. *J. Chem. Soc., Dalton Trans.* **1977**, 986.
(7) (a) Hauser, U.; Oestreich, V.; Rohrweck, H. D. *Z. Phys. A* **1977**, *280*, 17. (b) Hauser, U.; Oestreich, V.; Rohrweck, H. D. *Z. Phys. A* **1977**, *280*, 125.
(8) Zöllner, H.; Woike, Th.; Krasser, W.; Haussühl, S. *Z. Kristallogr.* **1989**, *188*, 139.
(9) Manoharan, P. T.; Gray, H. B. *J. Am. Chem. Soc.* **1965**, *87*, 3340.
(10) (a) Woike, Th.; Krasser, W.; Bechthold, P. S.; Haussühl, S. *Solid State Commun.* **1983**, *45*, 499. (b) Woike, Th.; Krasser, W.; Bechthold, P. S.; Haussühl, S. *Phys. Rev. Lett.* **1984**, *53*, 1767.
(11) Woike, Th.; Krasser, W.; Zöllner, H.; Kirchner, W.; Haussühl, S. *Z. Phys. D* **1993**, *25*, 351.
(12) Enemark, J. H.; Feltham, R. D. *Coord. Chem. Rev.* **1974**, *13*, 339.
(13) Rüdlinger, M.; Schefer, J.; Chevrier, G.; Furer, N.; Güdel, H. U.; Haussühl, S.; Heger, G.; Schweiss, P.; Vogt, T.; Woike, Th.; Zöllner, H. *Z. Phys. B* **1991**, *83*, 125.
(14) Güida, J. A.; Piro, O. E.; Schaiquevich, P. S.; Aymonino, P. J. *Solid State Commun.* **1997**, *101*, 471.
(15) Güdel, H. U. *Chem. Phys. Lett.* **1990**, *175*, 262.
(16) Woike, Th.; Kirchner, W.; Kim, H.; Haussühl, S.; Rusanov, V.; Angelov, V.; Ormandjiev, S.; Bonchev, T.; Schroeder, A. N. F. *Hyperfine Interact.***1993**, *7*, 265.
(17) Kruschel, G. *Elektronenspinresonanz an einem Metastable Zustand im Komplex* $[Fe(CN)_5]^{3-}$. Dissertation, Darmstadt, 1984.
(18) Pressprich, M. R.; White, M. A.; Vekhter, Y.; Coppens, P. *J. Am. Chem. Soc.* **1994**, *116*, 5233.
(19) Harlow, R. L. *J. Res. NIST* **1996**, *101*, 327.
(20) Fomitchev, D. V.; Coppens, P. *Inorg. Chem.* **1996**, *35*, 7021.
(21) Morioka, Y.; Takeda, S.; Tomizawa, H.; Miki, E. *Chem. Phys. Lett.* **1998**, *292*, 625.
(22) Chacón Villalba, M. E.; Güida, J. A.; Varetti, E. L.; Aymonino, P. J. *Spectrochim. Acta A* **2001**, *57*, 367.
(23) (a) Rüdlinger, M.; Schefer, J.; Vogt, T.; Woike, Th.; Haussühl, S.; Zöllner, H. *Physica B* **1992**, *180−181*, 293. (b) Schefer, J.; Woike, Th; Haussühl, S.; Fernandez Diaz, M. T. *Z. Kristallogr.* **1997**, *212*, 29.
(24) Terrile, C.; Nascimento, O. R.; Moraes, I. J.; Castellano, E. E.; Piro, O. E.; Güida, J. A.; Aymonio, P. J. *Solid State Commun.* **1990**, *73*, 481.
(25) Side-on geometries have been predicted for the ground states of $Sc(NO)^+$, $Ti(NO)^+$, and $V(NO)^+$. See: Thomas, J. L. C.; Bauschlicher, C. W.; Hall, M. B. *J. Phys. Chem. A* **1997**, *101*, 8530.
(26) Manoharan, P. T.; Hamilton, W. C. *Inorg. Chem.* **1963**, *2*, 1043.

(27) Fenske, R. F.; DeKock, R. L. *Inorg. Chem.* **1972**, *11*, 437.
(28) Hollauer, E.; Olabe, J. A. *J. Braz. Chem. Soc.* **1997**, *8*, 495.
(29) Bottomley, F.; Grein, F. *J. Chem. Soc., Dalton Trans.* **1980**, 1359.
(30) Gołębiewski, A.; Wasielewska, E. *J. Mol. Struct.* **1980**, *67*, 183.
(31) Wasielewska, E. *Inorg. Chim. Acta* **1986**, *113*, 115.
(32) Estrin, D. A.; Baraldo, L. M.; Slep, L. D.; Barja, B. C.; Olabe, J. A.; Paglieri, L.; Corongiu, G. *Inorg. Chem.* **1996**, *35*, 3897.
(33) Delley, B.; Schefer, J.; Woike, Th. *J. Chem. Phys.* **1997**, *107*, 10067.
(34) Boulet, P.; Buchs, M.; Chermette, H.; Daul, C.; Gilardoni, F.; Rogemond, F.; Schläpfer, C. W.; Weber, J. *J. Phys. Chem. A* **2001**, *105*, 8991.
(35) Novozhilova, I.; Coppens, P. Unpublished results.
(36) Vosko, S. H.; Wilk, L.; Nusair, M. *Can. J. Phys.* **1980**, *58*, 1200.
(37) Perdew, J. P.; Wang, Y. *Phys. Rev. B* **1992**, *45*, 13244.
(38) Wang, Y.; Perdew, J. P. *Phys. Rev. B* **1991**, *44*, 13298.
(39) Boulet, P.; Buchs, M.; Chermette, H.; Daul, C.; Furet, E.; Gilardoni, F.; Rogemond, F.; Schläpfer, C. W.; Weber, J. *J. Phys. Chem. A* **2001**, *105*, 8999.
(40) Becke, A. D. *Phys. Rev. A* **1988**, *38*, 3098.
(41) Perdew, J. P.; Wang, Y. *Phys. Rev. B* **1986**, *33*, 8800.
(42) Schaiquevich, P. S.; Güida, J. A.; Aymonino, P. J. *Inorg. Chim. Acta* **2000**, *303*, 277.
(43) Boulet, P.; Chermette, H.; Weber, J. *Inorg. Chem.* **2001**, *40*, 7032.
(44) Zhou, M.; Andrews, L. *J. Phys. Chem. A* **2000**, *104*, 3915.
(45) Krim, L.; Manceron, L.; Alikhani, M. E. *J. Phys. Chem. A* **1999**, *103*, 2592.
(46) Woike, Th.; Zöllner, H.; Krasser, W.; Haussühl, S. *Solid State Commun.* **1990**, *73*, 149.
(47) Woike, Th.; Haussühl, S. *Solid State Commun.* **1993**, *86*, 333.
(48) Guida, J. A.; Piro, O. E.; Aymonino, P. J. *Inorg. Chem.* **1995**, *34*, 4113.
(49) Ookubo, K.; Morioka, Y.; Tomizawa, H.; Miki, E. *J. Mol. Struct.* **1996**, *379*, 241.
(50) (a) Woike, Th.; Haussühl, B.; Sugg, B.; Rupp, R. A.; Beckers, J.; Imlau, M.; Schieder, R. *Appl. Phys. B* **1996**, *63*, 243. (b) Woike, Th.; Imlau, M.; Haussühl, S.; Rupp, R. A.; Schieder, R. *Phys. Rev. B* **1998**, *58*, 8411. (c) Imlau, M.; Woike, Th.; Schieder, R.; Rupp, R. A. *Phys. Rev. Lett.* **1999**, *82*, 2860. (d) Imlau, M.; Woike, Th.; Schieder, R.; Rupp, R. A. *Europhys. Lett.* **2001**, *53*, 471. (e) Imlau, M.; Haussuhl, S.; Woike, Th.; Schieder, R.; Angelov, V.; Rupp, R. A.; Schwarz, K. *Appl. Phys. B* **1999**, *68*, 877.
(51) Fomitchev, D. V.; Coppens, P. *Comments Inorg. Chem.* **1999**, *21*, 131.
(52) Cotton, F. A.; Wilkinson, G. *Advanced Inorganic Chemistry*; Wiley-Interscience Publication: New York, 1988.
(53) Mercer, E. E.; McAllister, W. A.; During, J. R. *Inorg. Chem.* **1966**, *5*, 1881.
(54) Fomitchev, D. V. *Study of Light-Induced Linkage Isomers in Transition Metal Nitrosyls*. Ph.D. Dissertation. State University of New York at Buffalo. 1998.
(55) Morioka, Y.; Ishikawa, A.; Tomizawa, H.; Miki, E. *J. Chem. Soc., Dalton Trans.* **2000**, 781.
(56) Kim, C. D.; Novozhilova, I.; Goodman, M. S.; Bagley, K. A.; Coppens, P. *Inorg. Chem.* **2000**, *39*, 5791.
(57) Zöllner, H.; Krasser, W.; Woike, Th.; Haussuehl, S. *Chem. Phys. Lett.* **1989**, *161*, 497.
(58) Fomitchev, D. V.; Novozhilova, I.; Coppens, P. *Tetrahedron* **2000**, *56*, 6813.
(59) Ohashi, Y.; Yanagi, K.; Kurihara, T.; Sasada, Y.; Ohgo, Y. *J. Am. Chem. Soc.* **1981**, *103*, 5805.
(60) Kawano, M.; Ishikawa, A.; Morioka, Y.; Tomizawa, H.; Miki, E.; Ohashi, Y. *J. Chem. Soc., Dalton Trans.* **2000**, 2425.
(61) Da Silva, S. C.; Franco, D. W. *Spectrochim. Acta A* **1999**, *55*, 1515.
(62) Guida, J. A.; Piro, O. K.; Aymonino, P. J. *Inorg. Chem.* **1995**, *34*, 4113.
(63) Novozhilova, I. *Application of Density Functional Theory to the Study of Ground and Photoinduced Metastable States of Selected Transition Metal Nitrosyl Complexes*. M.A. Thesis, State University of New York at Buffalo, 2001.
(64) Lyne, P. D.; Mingos, D. M. P. *J. Chem. Soc., Dalton Trans.* **1995**, 1635.
(65) Gorelsky, S. I.; Lever, A. B. P. *Int. J. Quantum Chem.* **2000**, *80*, 636.
(66) Gorelsky, S. I.; Da Silva, S. C.; Lever, A. B. P.; Franco, D. W. *Inorg. Chim. Acta* **2000**, *300*−*302*, 698.
(67) Becke, A. D. *J. Chem. Soc.* **1993**, *98*, 5648.
(68) Woike, Th.; Imlau, M.; Angelov, V.; Schefer, J.; Delley, B. *Phys. Rev. B* **2000**, *61*, 249.
(69) Blaha, P.; Schwartz, K.; Faber, W.; Luitz, J. *Hyperfine Interact.* **2000**, *126*, 389−395.
(70) Gomez, J. A.; Guenzburger, D. *Chem. Phys.* **2000**, 73.
(71) Cheng, L.; Richter-Addo, G. B. Binding and Activation of Nitric Oxide by Metalloporphyrins and Heme. In *The Porphyrin Handbook*; Kadish, K. M., Smith, K. M., Guilard, R., Eds.; Academic Press: New York, 2000; Vol. 4, pp 219−291.
(72) Walda, K. N.; Liu, X. Y.; Sharma, V. S.; Magde, D. *Biochemistry* **1994**, *33*, 2198.
(73) (a) Carlson, M. L.; Regan, R.; Elber, R.; Li, H.; Phillips, G. N.; Olson, J. S.; Gibson, Q. H. *Biochemistry* **1994**, *33*, 10597. (b) Olson, J. S.; Phillips, G. N. *J. Biol. Chem.* **1996**, *271*, 17593.
(74) Zavarine, I. S.; Kini, A. D.; Morimoto, B. H.; Kubiak, C. P. *J. Phys. Chem. B* **1998**, *102*, 7287.
(75) Morlino, E. A.; Rodgers, M. A. *J. Am. Chem. Soc.* **1996**, *118*, 11798.
(76) Ford, P. C.; Bourassa, J.; Miranda, K.; Lee, B.; Lorkovic, I.; Boggs, S.; Kudo, S.; Laverman, L. *Coord. Chem. Rev.* **1998**, *171*, 185.
(77) Hoshino, M.; Laverman, L.; Ford, P. C. *Coord. Chem. Rev.* **1999**, *187*, 75.
(78) Miller, L. M.; Pedraza, A. J.; Chance, M. R. *Biochemistry* **1997**, *36*, 12199.
(79) Weichsel, A.; Andersen, J. F.; Roberts, S. A.; Montfort, W. R. *Nature Struct. Biol.* **2000**, *7*, 551.
(80) Fomitchev, D. V.; Coppens, P.; Li, T.; Bagley, K. A.; Chen, L.; Richter-Addo, G. B. *Chem. Commun.* **1999**, 2013.
(81) Nakamoto, K. *Infrared and Raman Spectra of Inorganic and Coordination Compounds, Part B*; John Wiley and Sons: New York, 1997; p 149.
(82) (a) Li, X. Y.; Czernuszewicz, R. S.; Kincaid, J. R.; Stein, P.; Spiro, T. G. *J. Phys. Chem.* **1990**, *94*, 47. (b) Piffat, C.; Melamed, D.; Spiro, T. G. *J. Phys. Chem.* **1993**, *97*, 7441.
(83) Kitagawa, T.; Ozaki, Y. *Struct. Bonding* **1987**, *64*, 71.
(84) Spiro, T. G. In *Iron Porphyrin*; Lever, A. B. P., Gray, H. B., Eds.; Addison-Wesley: Reading, MA, 1983; Vol. 2, pp 91−152.
(85) Cheng, L.; Novozhilova, I.; Kim, C.; Kovalevsky, A.; Bagley, K. A.; Coppens. P.; Richter-Addo, G. B. *J. Am. Chem. Soc.* **2000**, *122*, 7142.
(86) Ellison, M. K.; Scheidt, W. R. *J. Am. Chem. Soc.* **1997**, *119*, 7404.
(87) Scheidt, W. R.; Duval, H. F.; Neal, T. J.; Ellison, M. K. submitted.
(88) Scheidt, W. R.; Ellison, M. K. *Acc. Chem. Res.* **1999**, *32*, 350.
(89) Wondimagegn, T.; Ghosh, A. *J. Am. Chem. Soc.* **2001**, *123*, 5680.
(90) Ghosh, A.; Wondimagegn, T. *J. Am. Chem. Soc.* **2000**, *122*, 8101.
(91) (a) Allen, A. D.; Senoff, C. V. *J. Chem. Soc., Chem. Commun.* **1965**, 621. (b) Allen, A. D.; Bottomley, F.; Harris, R. O.; Reinsalu, V. P.; Senoff, C. V. *J. Am. Chem. Soc.* **1967**, *89*, 5595.
(92) Busetto, C.; D'Alfonso, A.; Maspero, F.; Perego, G.; Zazzetta, A. *J. Chem. Soc., Dalton Trans.* **1977**, 1828.
(93) Thorn, D. L.; Tulip, T. H.; Ibers, J. A. *J. Chem. Soc., Dalton Trans.* **1979**, 2022.
(94) Armor, J. N.; Taube, H. *J. Am. Chem. Soc.* **1970**, *92*, 2560.
(95) (a) Ozin, G. A.; Vander Voet, A. *Can. J. Chem.* **1973**, *51*, 637. (b) Ozin, G. A.; Vander Voet, A. *Acc. Chem. Res.* **1973**, *6*, 313.
(96) (a) Bercaw, J. E.; Rosenberg, E.; Roberts, J. D. *J. Am. Chem. Soc.* **1974**, *96*, 612. (b) Gynane, M. J. S.; Jeffery, J.; Lappert, M. F. *J. Chem. Soc., Chem. Commun.* **1978**, 34. (c) Schrock, R. R.; Glassman, T. E.; Vale, M. G., Kol, M. *J. Am. Chem. Soc.* **1993**, *115*, 1760. (d) Cusanelli, A.; Sutton, D. *Organometallics* **1996**, *15*, 1457.
(97) Mortensen, J. J.; Hammer, B.; Nørskov, J. K. *Phys. Rev. Lett.* **1998**, *80*, 4333.
(98) Fomitchev, D. V.; Bagley, K. A.; Coppens, P. *J. Am. Chem. Soc.* **2000**, *122*, 532.
(99) Jørgensen, S. M. *Z. Anorg. Chem.* **1898**, *5*, 168.
(100) Adell, B. *Z. Anorg. Allg. Chem.* **1955**, *279*, 219.
(101) Wendlandt, W. W.; Woodlock, J. H. *J. Inorg. Nucl. Chem.* **1965**, *27*, 259.
(102) Balzani, V.; Ballardini, R.; Sabbatini, N.; Moggi, L. *Inorg. Chem.* **1968**, *7*, 1398.
(103) Grenthe, I.; Nordin, E. *Inorg. Chem.* **1979**, *18*, 1869.
(104) Grenthe, I.; Nordin, E. *Inorg. Chem.* **1979**, *18*, 1109.
(105) Heyns, A. M.; de Waal, D. *Spectrochim. Acta A* **1989**, *45*, 905.
(106) Kubota, M.; Ohba, S. *Acta Crystallogr. B* **1992**, *48*, 627.
(107) Masciocchi, N.; Kolyshev, A.; Dulepov, V.; Boldyreva, E.; Sironi, A. *Inorg. Chem.* **1994**, *33*, 2579.
(108) Johnson, D. A.; Pashman, K. A. *Inorg. Nucl. Chem. Lett.* **1975**, *11*, 23.
(109) Gordon, G. M.; Feltham, R. D.; Turner, J. T. *J. Phys. Chem.* **1991**, *95*, 2889.
(110) Sabbatini, N.; Moggi, L.; Varani, G. *Inorg. Chim. Acta* **1971**, *5*, 469.
(111) Scandola, F.; Bartocci, C.; Scandola, M. A. *J. Phys. Chem.* **1974**, *78*, 572.
(112) Scandola, M. A.; Bartocci, C.; Scandola, F.; Carasitti, V. *Inorg. Chim. Acta* **1978**, *28*, 151.
(113) Natarajan, P.; Radhakrishnan, A. *J. Chem. Soc., Dalton Trans.* **1982**, 2403.
(114) Gillard, R. D.; De Jesus, J. D. P. *J. Chem. Soc., Dalton Trans.* **1984**, 1895.
(115) Johnson, D. A.; Dew, V. C. *Inorg. Chem.* **1979**, *18*, 3273.
(116) Kovalevsky, A.; Coppens, P.; Bagley, K. A. *Abstracts of Papers*. 222nd National Meeting of the American Chemical Society, Chicago, IL, Fall 2001; American Chemical Society: Washington, DC, 2001; Paper no. 78. Kovalevsky, A.; Coppens, P. To be published.

(117) Kita, M.; Yamanari, K.; Shimura, Y. *Chem. Lett.* **1984**, 297.
(118) Murata, M.; Kojima, M.; Hioki, A.; Miyagawa, M.; Hirotsu, M.; Nakajima, K.; Kita, M.; Kashino, S.; Yoshikawa, Y. *Coord. Chem. Rev.* **1998**, *174*, 109.
(119) Burmeister, J. *Coord. Chem. Rev.* **1990**, *105*, 77.
(120) Buckingham, D. A. *Coord. Chem. Rev.* **1994**, *135*−*136*, 587.
(121) Wei, H.-H.; Ho, L. Z. *Inorg. Chem.* **1984**, *23*, 624.
(122) Smith, M. K.; Gibson, J. A.; Young, C. G.; Broomhead, J. A.; Junk, P. C.; Keene, F. R. *Eur. J. Inorg. Chem.* **2000**, 1365.
(123) Rack, J. J.; Winkler, J. R.; Gray, H. B. *J. Am. Chem. Soc.* **2001**, *123*, 2432.
(124) Alway, D. G.; Barnett, K. W. *J. Organomet. Chem.* **1975**, *99*, C52.
(125) Houlding, V. H.; Mäcke, H.; Adamson, A. W. *Inorg. Chem.* **1981**, *20*, 4279.
(126) Alessio, E.; Faleschini, P.; o Santi, A. S.; Mestroni, G.; Calligaris, M. *Inorg. Chem.* **1993**, *32*, 5756.
(127) Akhter, F. M. D.; Hirotsu, M.; Sugimoto, I.; Kojima, M.; Kashino, S.; Yoshikawa, Y. *Bull. Chem. Soc. Jpn.* **1996**, *69*, 643 (and references therein).
(128) Schaftenaar, G.; Noordik, J. H. *J. Comput.-Aided Mol. Design* **2000**, *14*, 123.
(129) Volkov, A. V. *ADF2MOLDEN*; State University of New York at Buffalo, 1999.

CR000031C